NASA-CR-195515

NASA ADVANCED DESIGN PROGRAM

Design and Analysis of a Radio-Controlled Flying Wing Aircraft

NASW-4435

IN-05-CR
204234
P- 100

A Major Qualifying Project
Submitted to the Faculty
of the

WORCESTER POLYTECHNIC INSTITUTE

in Partial Fullfillment of the Requirements
for the
Degree of Bachelor of Science
Submitted on May 3, 1993

(NASA-CR-195515) NASA ADVANCED DESIGN PROGRAM. DESIGN AND ANALYSIS OF A RADIO-CONTROLLED FLYING WING AIRCRAFT (Worcester Polytechnic Inst.) 100 p

N94-24589

Unclas

G3/05 0204234

ABSTRACT

The development of new high-speed, high-capacity public air transportation is one of the challenges facing commercial aviation today. One possible solution to this challenge is a supersonic oblique flying wing aircraft. This project involves the design and construction of a radio-controlled model of a flying wing aircraft as a means of examining some of the aircraft's unique problems, especially its natural instability. The different areas of stability, controls, aerodynamics, structures, and propulsion are analyzed in the context of the aircraft as a whole. The design relies heavily upon computer modeling and analysis to overcome the technical challenges encountered. Since the size of the model prohibits the use of automatic control systems, the wing is designed to be as inherently stable as possible, and an airfoil is designed to provide the necessary characteristics. Finally, the optimum design is chosen and constructed using composite materials.

ACKNOWLEDGEMENTS

A design endeavor such as this involves the efforts of many people outside the immediate project group. The members of the project group therefore wish to extend their gratitude to the following people for their technical support and guidance during the project:

Professor Andreas Alexandrou

Professor William Durgin

Professor David Olinger

Paul Crivelli

NASA/USRA

Foam Technologies especially Mark Blais

Arthur Lavallee of Mild to Wild Hobby Shop

Scaled Composites

Kress Jets, Inc.

Bob Taylor

EXECUTIVE SUMMARY

The main challenge of this project was to design an aircraft that will achieve stability while flying without a horizontal tail. The project focused on both the design, analysis and construction of a remotely piloted, elliptical shaped flying wing.

The design team was composed of four sub-groups each of which dealt with the different aspects of the design, namely aerodynamics, stability and control, propulsion and structures. Each member of the team initially researched the background information pertaining to specific facets of the project. Since previous work on this topic was limited, most of the focus of the project was directed towards developing an understanding of the natural instability of the aircraft.

Once the design team entered the conceptual stage of the project, a series of compromises had to be made to satisfy the unique requirements of each sub-group. As a result of the numerous calculations and iterations necessary, computers were utilized extensively. In order to visualize the design and layout of the wing, engines and control surfaces, a solid modeling package was used to evaluate optimum design placements.

When the design was finalized, construction began with the help of all the members of the project team. The nature of the carbon composite construction process demanded long hours of manual labor. The assembly of the engine systems also required precision hand work.

The final product of this project is the *Elang*, a one-of-a-kind remotely piloted aircraft of composite construction powered by two ducted fan engines.

TABLE OF CONTENTS

TABLE OF CONTENTS (continued)

LIST OF FIGURES AND TABLES

NOMENCLATURE

AR	aspect ratio
c	chord length
C_d	section drag coefficient
C_D	total drag coefficient
C_{Db}	coefficient of drag directed back
C_{Dd}	coefficient of drag directed down
C_{Di}	induced drag coefficient
C_{Do}	parasitic drag coefficient
$C_{D,LP}$	leakage/protuberance drag coefficient
C_f	skin friction coefficient
C_l	section lift coefficient
C_L	wing lift coefficient
C_{Lb}	coefficient of lift directed back
C_{Lu}	coefficient of lift directed upward
C_M	coefficient of moment
C_{Mac}	coefficient of moment about the aerodynamic center
FF	component form factor
M_r	rolling moment
Q	interference effects factor
S_{ref}	reference (planform) area
S_{wet}	wetted area
v_∞	flight speed
w_e	weight of each engine
w_m	weight of the mass
w_w	weight of the wing
x_{ac}	location of the aerodynamic center along the x-axis
x_{cg}	location of the center of gravity along the x-axis
x_{ecg}	location of the center of gravity of each engine along the x-axis
x_{mass}	location of the center of gravity of added mass along the x-axis
x_{wcg}	location of the center of gravity of the wing along the x-axis
y_{ac}	location of the aerodynamic center along the y-axis
y_{cg}	location of the center of gravity along the y-axis
y_{ecg}	location of the center of gravity of each engine along the y-axis
y_{mass}	location of the center of gravity of added mass along the y-axis
y_{wcg}	location of the center of gravity of the wing along the y-axis
α	angle of attack
ρ	air density

CHAPTER ONE: INTRODUCTION

The development of new high-speed, high-capacity public air transportation is one of the challenges facing commercial aviation as our society enters the twenty-first century. One possible solution to this challenge is a supersonic oblique flying wing aircraft. For instance, such an aircraft could carry as many as 500 passengers travelling at 1100 miles per hour, enabling transportation from New York to Los Angeles to be completed in under three hours (Jones, "Technical Note", p. 106). This concept was initially proposed by Robert T. Jones in 1958 (p. 104) but was not believed to be a feasible design due to structural and stability considerations. Today, however, the technology exists to overcome these challenges.

Since the full scope of such an endeavor involves numerous difficulties, simplicity must be used to surmount these problems by examining the different aspects individually. With this approach in mind, a simplified design was developed and analyzed which studied the stability, structural and aerodynamic issues of an unswept elliptically shaped flying wing. Even the nature of this type of aircraft provides design obstacles which must be faced in order to eventually apply the solutions to a full scale aircraft.

The result of these efforts is the *Elang*. A Figure 1.1 (also Appendix G) shows the final design. Due to the unique design requirements, the development of an original airfoil was necessary, resulting in the HPRS 33 airfoil section. The wing has a root chord length of 45.5 cm and a span of approximately 2.5 m, with an aspect ratio of 7. The planform area is elliptically shaped with a straight quarter-chord line according to,

$$c(z) = c_0\sqrt{1-(\frac{2z}{b})^2} = 0.455\sqrt{1-(\frac{2z}{2.5})^2} \qquad [1.1]$$

The induced drag is minimized by using an elliptical shape giving a total drag coefficient of 0.02208. The flying wing is at a geometric attack angle of 4 degrees and as a results generates a lift coefficient of 0.4355 at cruise speed of 15 m/s. The lift to drag ratio is therefore 19.69.

The main control surfaces include two ailerons and one elevator which are used to stabilize the aircraft in flight. The ailerons are located on each end outboard the engines, occupying 2.9 percent of the wing planform area. The elevator area is 13 percent of the wing planform area.

Two vertical tails are utilized, each located on the rear portion of the engine ducts. The airfoil section is the symmetric SD 8020 airfoil. The vertical stabilizers each have an effective area of 0.10716 m^2 to provide yaw control. Rather large rudder surfaces were purposely employed to ensure adequate control. Only vertical tails are used, since by nature the flying wing design does not contain a horizontal tail.

A propulsion system was chosen which provides ample thrust and relatively clean aerodynamics. The system consists of two ducted fan engines, each placed 57 cm from the root chord. Operating at 22000 rpm, each engine provides 15.60 N of thrust. One centrally located fuel tank supplies both engines.

The wing structure is designed to be composed of a foam core wrapped with a skin of carbon fiber and epoxy. This provides a relatively lightweight structure that can still withstand sizable loads.

The main focus of this project involves the design and construction of a radio-controlled model of an elliptical flying wing as a means of examining some of the aircraft's unique problems, especially its natural instability. The design relies heavily upon computer modeling and analysis to overcome the technical challenges encountered. Since the size of the model prohibits the use of automatic control systems, the wing is designed to be as inherently stable as possible, and an airfoil is designed to provide the necessary characteristics. Finally, the optimum design is chosen and constructed using composite materials. To achieve this final product the group was divided into four sub-groups, dealing with aerodynamics, controls and stability, structures and propulsion. In the following chapters, the analysis of each sub-group and explanations for its results are presented.

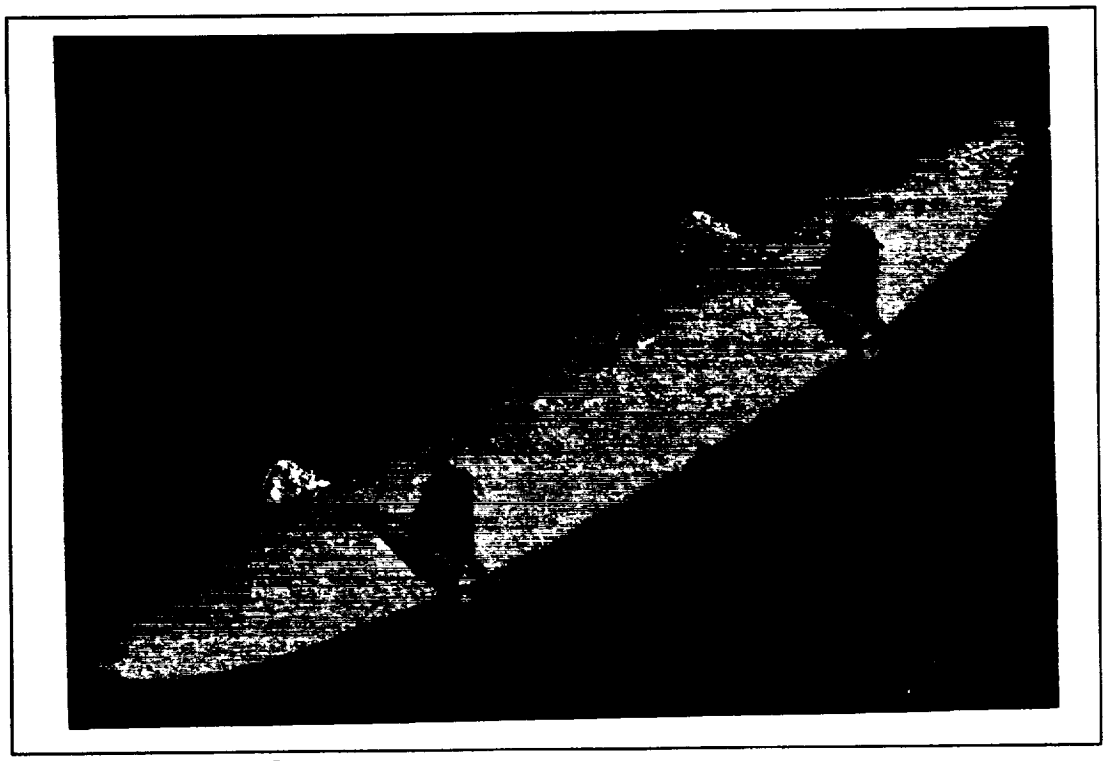

Figure 1.1: The *Elang*

CHAPTER TWO: STABILITY AND CONTROL SURFACES

2.1 Stability

Stability is defined as the ability of an airplane to fly straight with its wings level, and remain in equilibrium without pilot assistance. It can be divided into two categories, static and dynamic, and can be analyzed along three axes, pitch, roll, and yaw.

Static stability deals with the natural ability of an aircraft to create a restoring moment after a disturbance, and return towards its initial equilibrium position. For instance, when in straight and level flight a statically stable airplane encounters a gust of wind, it generates a moment to counteract the perturbance. This type of stability does not give any information on how long it takes to return to its original position, and does not even insure that the plane will return exactly to its equilibrium state. A dynamic stability analysis must be performed in order to obtain this information.

Dynamic stability concerns the motion of the aircraft after the disturbance. In order for the aircraft to be dynamically stable, it must return to the equilibrium position within a certain amount of time, and thus damping is required. If an aircraft is dynamically stable, it will also be statically stable, but the reverse is not necessarily true.

There are three axes about which stability must be achieved. The rotations are about the conventional x, y, and z axes, and the motions are designated as roll, pitch, and yaw, respectively (Figure 2.1). These motions can be separated into two distinct groups, lateral and longitudinal. Lateral motions consist of rolling, yawing, and

sideslipping. Longitudinal motions denote the movement along the aircraft's flight path, its vertical movement, and pitching.

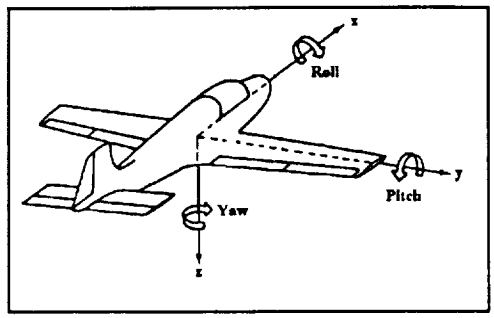

Figure 2.1: Axes of Rotation (Shevell, Fundamentals of Flight)

The major difficulty in stabilizing a flying wing is along the pitch axis. In conventional designs, a horizontal tail offsets the moments generated by the wing and fuselage. However, a flying wing does not have a horizontal tail. Consequently, an alternative, more advanced method for stabilizing the wing had to be utilized.

2.2 Stability Analysis

Throughout the analysis of stability and controls, the major tool that was utilized was the MATHCAD software package. By using this package, changes could be made to the iterative analysis easily and accurately. A listing of the MATHCAD results is located in Appendix A.

2.1.1 Pitch Stability

Conventional airfoils typically have a negative moment coefficient about the aerodynamic center. After analyzing a few such airfoils, it was found that to achieve static stability, the engines would have to be placed about a meter below the wing with some airfoils, and at the back of the wing for others. Since the back of the airfoil is the

thinnest part, and one meter is considerably too long for clearance, neither of these designs was acceptable. Thus, it was determined that an airfoil with a positive coefficient of moment about the aerodynamic center was needed. The positive moment causes the wing to have a natural tendency to pitch up. Therefore, the aerodynamics sub-group designed a new airfoil, through an extensive iterative process, which has a high lift to drag ratio along with a positive moment about the aerodynamic center.

Once the airfoil was selected, engine placement was used to obtain stability. The center of gravity for the design was calculated from the known values of the components. The weight of the wing and the location of its center of gravity along the x and y axes were generated using ARIES, a solid modeling computer program. These values were found to be 16 N, 0.209 m, and 0.00561 m respectively . The engines each weighed 5.719 N. A fixed mass of 0.5 kg was added to allow for the receiver, batteries, and other components. This mass was placed 5 cm from the leading edge along the chord line. The center of gravity of the design was calculated by Equations 2.1 and 2.2.

$$x_{cg} = \frac{x_{e_{cg}}(2*w_e) + x_{w_{cg}}*w_w + x_{mass}*w_{mass}}{2*w_e + w_w + w_{mass}} \qquad [2.1]$$

$$y_{cg} = \frac{y_{e_{cg}}(2*w_e) + y_{w_{cg}}*w_w + y_{mass}*w_{mass}}{2*w_e + w_w + w_{mass}} \qquad [2.2]$$

The moments about the center of gravity of the wing were analyzed, and the results led to Equation 2.3.

$$C_M = C_{M_{ac}} + C_{L_a}\frac{x_{cg}-x_{ac}}{c} - C_{L_b}\frac{y_{cg}-y_{ac}}{c} + C_{D_a}\frac{x_{cg}-x_{ac}}{c} - C_{D_b}\frac{y_{cg}-y_{ac}}{c} \qquad [2.3]$$

An iterative process was conducted with Equations 2.1 and 2.3, to determine the placement of the engines along the x-axis to ensure no inherent pitching moment. Equation 2.2 was used to find the location of the center of gravity of the wing along the y axis. Initially the y location of the engines was estimated to be six millimeters to begin the iteration of the design. The calculations were carried out with lift, drag, and moment data for the cruising angle of attack of 4 degrees.

A Moment Coefficient vs. Angle of Attack graph was generated to determine whether or not the wing was statically stable (Figure 2.2). By definition, an aircraft is statically stable if it satisfies Equation 2.4.

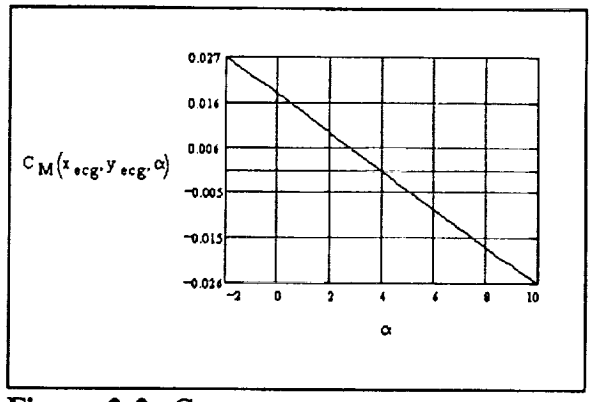

Figure 2.2: C_M vs. α

$$\frac{dC_M}{d\alpha} < 0 \qquad [2.4]$$

As seen in Figure 2.2, the negative slope ensures static stability along the pitch axis.

A major concern with this flying wing is the very low moment of inertia about the pitch axis, which is a result of the wing having no sweep angle. This low moment of inertia indicates that there is little time for a pilot to react to disturbances during flight. This problem, coupled with inability to guarantee exact placements and weights of the internal components of the wing, makes controllability extremely difficult for the

pilot. Therefore, a gyroscope system was included as a safety precaution. The gyroscope monitors deviations about the pitch axis, and makes constant adjustments by using the elevator. The gyroscope can be utilized at the pilot's discretion, depending on flight conditions.

In reference to dynamic stability, all available documentation depended on a horizontal tail to provide the damping. However, the flying wing has no horizontal tail. Thus, any damping that would occur to provide dynamic stability along the pitch axis is quite small. The lack of damping again showed the need for the gyroscope system.

2.2.2 Roll and Yaw Stability

The stabilities in the roll and yaw directions are linked closely together. Rotation along one of these axes induces an accompanying moment along the other axis. Due to the symmetry along the x and z axes, the problem of stability in these directions is not anticipated to be present. Additionally, if the wing does roll or yaw, the moment of inertia about these axes is substantial enough to create a rate of rotation that will provide ample time for the pilot to counter the deviations.

2.3 Control Surfaces

The control surfaces consist of an elevator, a pair of ailerons, and two rudders, which control motion along the pitch, roll, and yaw axes, respectively. The analysis was performed by considering the lift, drag, and moment characteristics of each control

surface. Each control system was analyzed independently of the other two. When sizing the control surfaces, they were purposely overdesigned, because the controllability of previous design projects has proven to be inadequate.

2.3.1 Elevator Analysis

The data for the elevator was obtained by modifying the inviscid code to provide new lift, drag, and moment coefficients when the control surface was deflected. The analysis was carried out through a range of angles from -30 to 30 degrees.

Once the data for the deflected area of the wing was procured, it was combined with the previous data for the remaining portion of the wing. From the combination of this data, a modified moment equation was developed. For these calculations, the length of the elevator was 1.4 meters at 18 percent of the cord length, resulting in an elevator area equal to 13 percent of the wing planform area. The moment is given as:

$$M_{def}=M_{ac}+L_u(x_{cg}-x_{ac})-L_b(y_{cg}-y_{ac})+D_d(x_{cg}-x_{ac})-D_b(y_{cg}-y_{ac})+M_{ac_{def}}$$

$$+L_{u_{def}}(x_{cg}-x_{ac_{def}})-L_{b_{def}}(y_{cg}-y_{ac_{def}})+D_d(x_{cg}-x_{ac_{def}})-D_{b_{def}}(y_{cg}-y_{ac_{def}}) \qquad [2.5]$$

where subscript def denote characteristics from the deflected portion.

Once the moments were determined, Newton's Second Law was applied to calculate the pitching acceleration of the wing. Figure 2.3

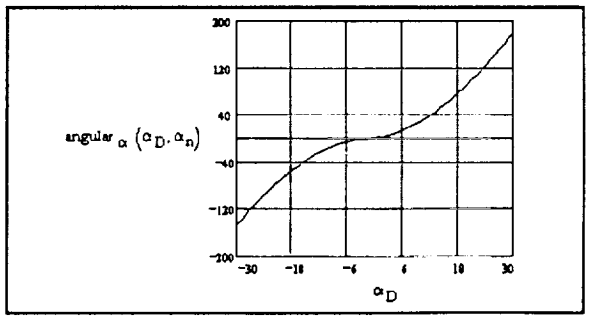

Figure 2.3: Angular Acceleration vs. Elevator Deflection Angle

shows the results of this analysis. The values for this acceleration ranged from negative to positive 200 rad/sec^2. These large accelerations develop because of the small moment of inertia of the wing about the pitch axis. From this data, it was decided that the gyroscope system should be utilized to aid the pilot in controlling the wing.

2.3.2 Aileron Analysis

The data from the elevator analysis was utilized in the analysis of the ailerons. This similarity occurs because the elevator and the ailerons deflect along the same axis, and both occupy 18 percent of the cord length. When examining the ailerons, it was decided that they would deflect at the same rate in opposite directions. For example, if one aileron was deflected up 10 degrees, the other one would deflect down 10 degrees. The rolling moment created by the drag from the rudders was neglected. The analysis produced the following moment equation.

$$M_r = L_{l_{ddf}} * z_{al} - L_{r_{ddf}} * z_{ar} \qquad [2.6]$$

Through iteration it was determined that the each aileron would have a length of 21.8 cm, which resulted in each aileron having 2.9 percent of the wing planform area. As with the elevator analysis, Newton's Second Law was applied to generate the angular acceleration about the roll axis of the wing. The acceleration ranged from negative to positive ten radians per second squared.

2.3.3 Vertical Stabilizer Design

The most important consideration in the design of the vertical stabilizers was the sizing. Due to the inherent control problems involved with a flying wing, it was imperative that the control surfaces be *over*sized to compensate for unpredictable stability failures. For most airplanes with a fuselage, tail and vertical rudder, the area required for the vertical tail is 3 to 5 percent of the entire planform area of the plane. The design of the flying wing called for an area of more than the typical percentage. Thus it was determined that the vertical tail area be 12 percent of the wing planform area. With a planform area of 0.893 m^2, the total vertical stabilizer area is 0.10716 m^2.

2.3.3 Rudder Analysis

The inviscid analysis that was used for the elevator and ailerons was also used to examine the rudders. Since there is such a small moment arm for the rudders, the size of each one is considerably larger than that of conventional designs. Two rudders were selected, for symmetry, and for structural considerations. Each rudder will have an area equal to 31.7 percent of the vertical stabilizer planform. This sizing is accomplished by having the height 21.3 cm, the root cord 17.2 cm, and the tip cord 8 cm.

In the analysis of the rudder, it was determined that each rudder would be deflected the same amount. The moment equations were developed separately for each rudder, and then summed. These expressions are given in Equations 2.7 and 2.8.

$$M_{lr} = D_r * z_{lr} - L_r(x_{lr} + x_{ac_r}) \quad [2.7]$$

$$M_{rr} = -D_r * z_{rr} - L_r(x_{rr} + x_{ac_r}) \quad [2.8]$$

Once the moment equations were developed, Newton's Second Law was applied to calculate the angular accelerations. A plot of these accelerations is given in Figure 2.4. In this graph, the maximum acceleration occurs close to zero. Since an inviscid analysis was used to obtain the data, drag effects are assumed small. In reality however, the drag effects will contribute greatly to the moment generated at large deflections.

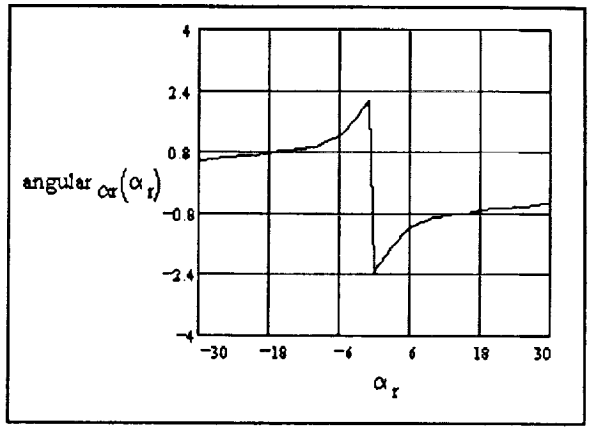

Figure 2.4: Rudder Angular Acceleration vs. Angle of Deflection

CHAPTER THREE: AERODYNAMIC DESIGN AND ANALYSIS

3.1 Introduction

This chapter discusses the aerodynamics of the aircraft, including the selection of the airfoil, airfoil characteristics, aerodynamic behavior of the aircraft, and the aerodynamic shape of the aircraft as a whole. The relationship between stability considerations and airfoil design is discussed thoroughly, since stability of the aircraft was of paramount importance. The analysis of the lift and drag characteristics for the aircraft turns out to be quite simple, since the entire aircraft is an elliptically-shaped wing.

3.2 Final Design

The final design is an elliptically shaped wing with a straight quarter chord line, the planform view of which is shown in Figure 3.1. The airfoil section used for the wing is the HPRS 33, a custom-designed airfoil. This airfoil, presented in Figure 3.2, is a 15-percent thick airfoil section with a reflexed camber. The wing has a span of 2.5 meters, an aspect ratio of 7, giving a root chord of 0.455 m and planform area S_{ref} of 0.893 m^2.

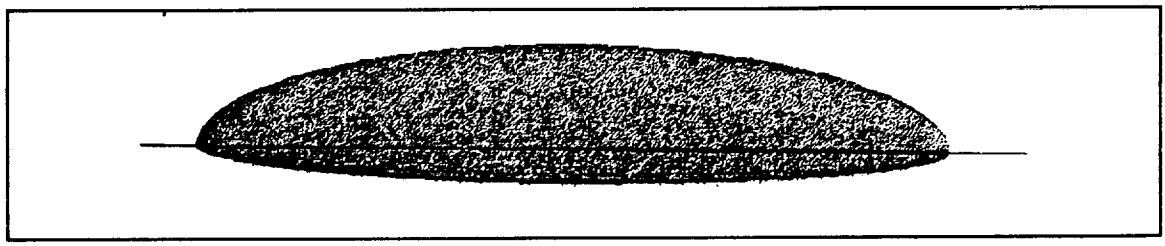

Figure 3.1: Planform of Wing

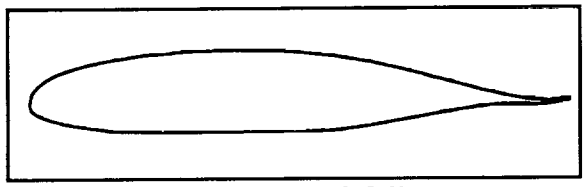

Figure 3.2: HPRS 33 Airfoil

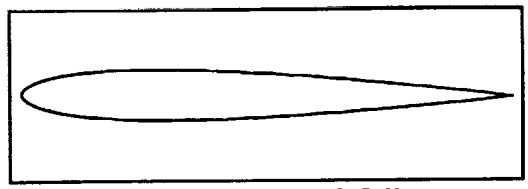

Figure 3.3: SD 8020 Airfoil

The two identical vertical tails each have a height of 0.213 meter, a root chord of 0.172 meter, and a tip chord of 0.08 meter. The trailing edge is unswept. The airfoil section used for the vertical tails is the SD8020, a 10-percent thick symmetric airfoil. This airfoil is shown in Figure 3.3.

3.3 Aerodynamic Requirements

The selection of the airfoil and the design of the wing shape were dictated by the consideration that the aircraft was to be a flying wing, which had to be controllable in flight by a single RC pilot. Three requirements in particular were: the need for relatively high lift and low drag; the requisite of static and dynamic stability; and structural rigidity as well as the location of engines, servos, and avionics.

One of the purposes of a flying wing configuration for a transport aircraft is to transport people and goods as efficiently as possible. Therefore the aircraft needs to have a high lift to drag ratio. A model of such an aircraft is no exception to this requirement. Since a finite wing of elliptical planform experiences a minimum induced drag, this shape was chosen for the flying wing. The wing quarter chord line is set to

be a straight line, visible in Figure 3.1. Having this configuration avoids further complications during construction.

The requirement of static and dynamic stability without a horizontal tail necessitates the use of an airfoil with special stability characteristics. While most airfoil sections have a negative moment coefficient, the flying wing application requires an airfoil with a positive moment coefficient, as discussed in Chapter 2. One way to accomplish this is to use an airfoil with a reflexed camber.

In addition, the wing must withstand the aerodynamic loads, particularly the twisting and bending loads. Since the aircraft has no fuselage, all components which include receiver and batteries, servos, and fuel tank, must be contained internally in the wing. These reasons led to the development of a thick airfoil, namely the HPRS 33 airfoil section.

3.4 Airfoil Design and Selection

3.4.1 Wing Airfoil Section

Since the flying wing has such special design requirements, it proved impossible to select an existing airfoil with the required lift, thickness, and moment characteristics. Therefore, it was necessary to develop an airfoil with the desired properties. To do this, the geometries of a thick high-lift airfoil and an airfoil with a positive moment coefficient were merged. A two-dimensional inviscid vortex panel code was utilized to calculate the lift, drag, and moment coefficients for the resulting airfoil. Points on the airfoil were

then changed and entered into the code in an iterative process until a satisfactory design was produced. The end result was the HPRS 33 airfoil, shown in Figure 3.2. Figure 3.4 presents the lift, drag, and moment coefficients versus angle of attack. Note that the drag coefficient is very low, since an inviscid approach was used.

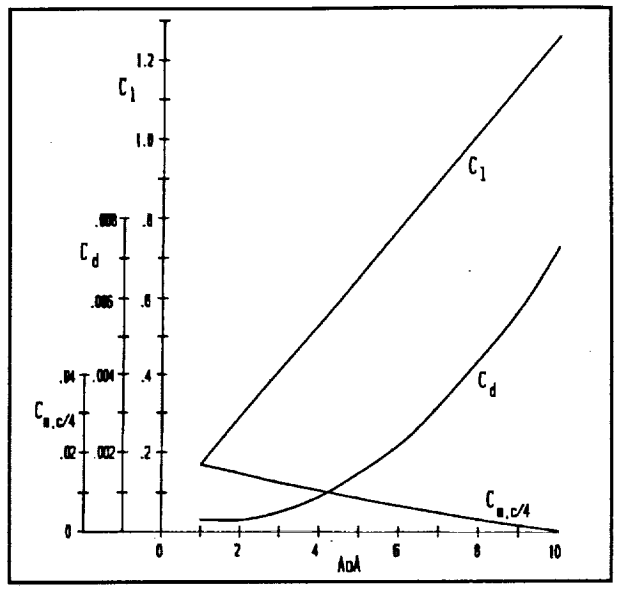

Figure 3.4: Aerodynamic Coefficients for HPRS 33

Appendix B lists the airfoil coordinates, as well as the lift, drag, and quarter-chord moment coefficients at various angles of attack for the HPRS 33 airfoil section.

3.4.2 Vertical Stabilizer Airfoil Section

The first consideration in the design of the vertical stabilizers was the shape of the airfoil to be used. After researching vertical tails on conventional airplanes, it was determined that a symmetrical airfoil was the best choice. By using a symmetrical airfoil, unnecessary moment forces caused by uneven lift distribution could be avoided. Research of thin symmetric airfoils provided the SD 8020 shape (see Figure 3.3). Appendix C lists the coordinates of the SD 8020 airfoil.

3.4.3 Vertical Stabilizer Sizing

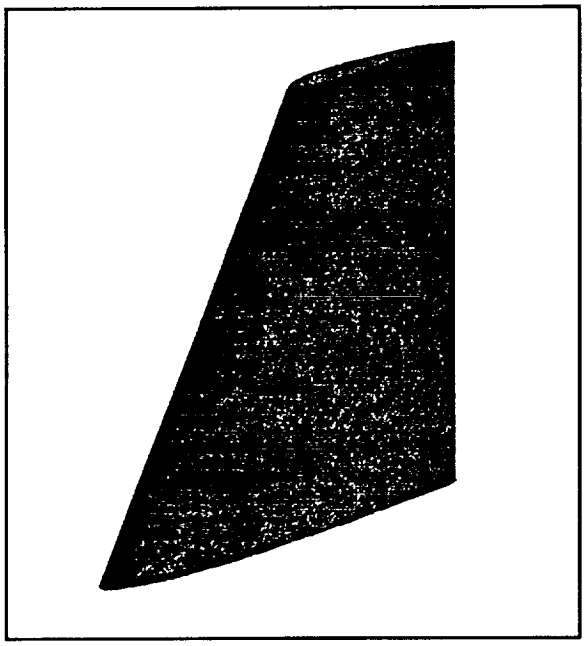

Figure 3.5: Vertical Tail

Sizing is the most important consideration in the design of the vertical stabilizer or tail as discussed in Chapter Two. With a given total vertical tail area of 0.10716 m^2,the final configuration of each vertical stabilizer consists of a root chord of 17.2 cm, a height of 21.3 cm, a tip chord of 8.0 cm and an aspect ratio of 0.85 (see Figure 3.5). These control surfaces provide adequate area for stabilization about the yaw axis.

3.5 Aerodynamic Calculations

The following is a very brief overview of the calculations performed to obtain theoretical lift and drag data for the aircraft.

3.5.1 Lift

To obtain theoretical lift values for the aircraft, the slope of the lift curve for the airfoil section first had to be obtained. This was obtained simply from the airfoil section data given in Appendix B; for the HPRS 33, $dc_l/d\alpha = 6.97$ per radian.

The lift curve slope for the finite wing is then given as

$$\frac{dC_L}{d\alpha} = \frac{2\pi AR}{2+\sqrt{(AR^2/\eta^2)\,(1+\tan^2\Lambda - M^2)}} \qquad [3.1]$$

The airfoil efficiency, η, is approximated as 1.0. The sweep angle, Λ, is zero, and the flight mach number is 0.044. Equation 3.1 thus results in $dc_L/d\alpha = 5$ per radian.

Integrating this expression gives

$$C_L = 5\alpha + constant \qquad [3.2]$$

The constant is obtained by using boundary conditions, which are approximated from the section lift curve slope: at $\alpha = 1°$, $c_l = 0.17$. Solving, the constant is found to be approximately 0.084. The lift curve slope for the entire wing is

$$C_L = 5\alpha + 0.084 \qquad [3.3]$$

where the angle of attack is in radians. The lift coefficient of the wing can thus be found for various angles of attack.

Knowing the lift coefficient, the lift force can be found at any speed for different angles of attack using the equation

$$L = \frac{1}{2}\rho V_\infty^2 C_L S_{ref} \qquad [3.4]$$

The lift of the aircraft at various angles of attack and various flight speeds is tabulated in Appendix D, using Equation 3.4. At cruise conditions (4° AoA, 15 m/s), the lift coefficient is 0.4355 and the total lift force is 53.55 N. The variation of available lift with velocity is shown in Figure 3.6.

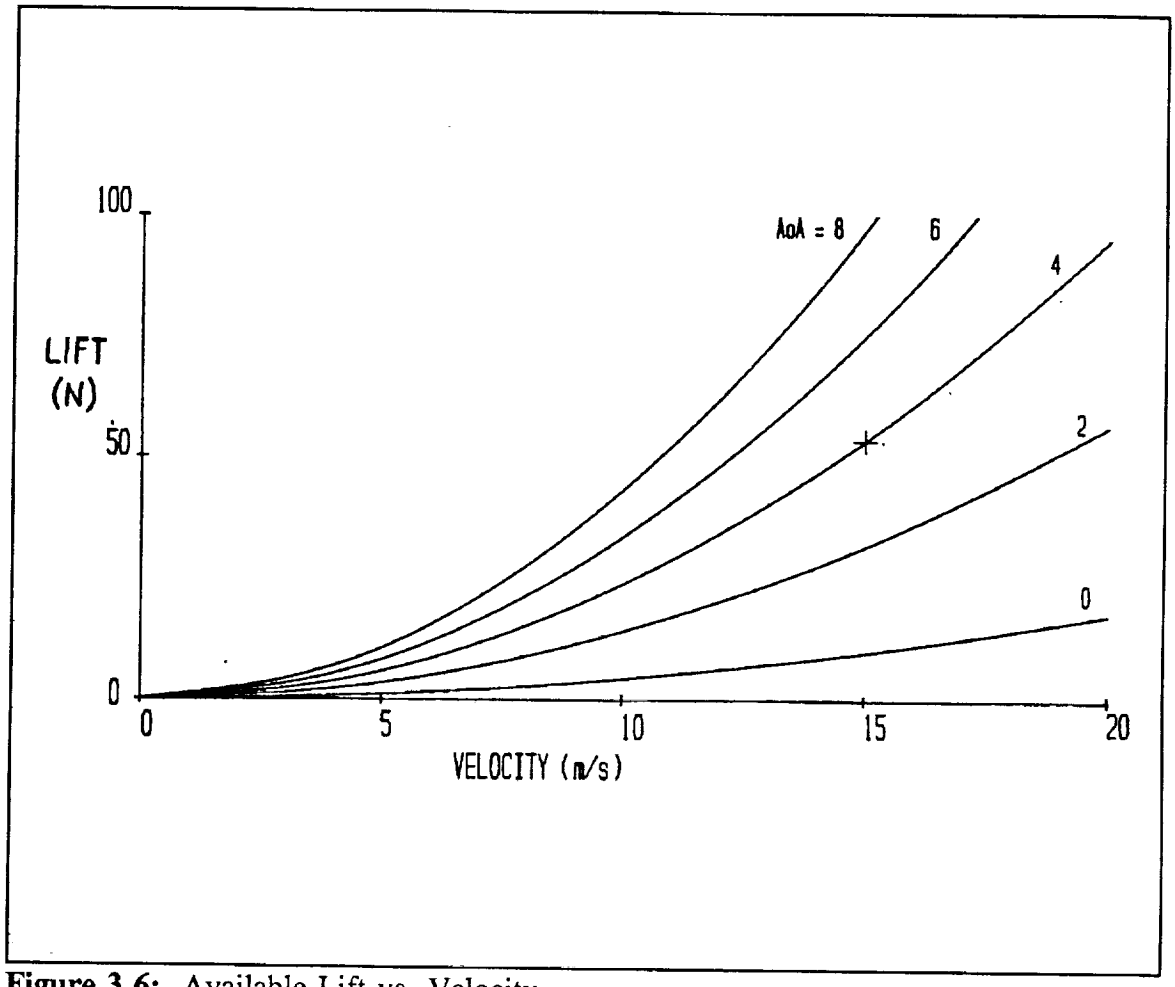

Figure 3.6: Available Lift vs. Velocity

3.5.2 Drag

Because the inviscid vortex panel code was not capable of providing accurate drag results, an empirical method suggested by Raymer was used.

This method depends upon the calculation of the parasitic drag, C_{Do}, based on equivalent skin friction coefficients C_{fc}, component form factors FF_c, interference effects Q_c, wetted area S_{wetc}, miscellaneous drags C_{Dmisc}, and estimated leakage and protuberance drag $C_{D,L\&P}$. The parasitic drag is calculated according to:

$$C_{Do} = \frac{\sum (C_{fc} FF_c Q_c S_{wetc})}{S_{ref}} + C_{D,misc} + C_{D,LP} \qquad [3.5]$$

(Raymer, pp. 280 -289). Appendix D lists the values of these parameters for each component of the aircraft, as well as the total parasitic drag for various flight conditions. At cruise conditions (4° AoA, 15 m/s), the approximate value of parasitic drag is C_{Do} = 0.01346.

The total induced drag, or drag due to lift, is given as

$$C_{Di} = KC_l^2 \qquad where \qquad K = \frac{1}{\pi ARe} \qquad [3.6]$$

For an elliptical planform, the Oswald span efficiency factor e is unity. Therefore, K = 0.04547, leading to a cruise C_{Di} of 0.008624. The total drag coefficient is simply the sum of the parasitic and induced drag coefficients, so that, at cruise,

$$C_D = C_{Do} + C_{Di} = 0.01346 + 0.008624 = 0.02208 \qquad [3.7]$$

The cruise drag force is therefore calculated at 2.72 N and the lift to drag ratio at cruise is 53.55/2.72 = 19.69.

CHAPTER FOUR: STRUCTURAL DESIGN AND ANALYSIS

4.1 Introduction

The structural design of the wing involved two primary objectives. The first was to reduce aeroelastic effects since this would alter the distribution of the forces along the wing and consequently alter the stability. Therefore the wing was designed to be as rigid as possible to minimize any bending. The second was to maintain manufacturability, since most of the construction was to be done by students using equipment available on campus.

One can describe the methods of the structures aspect of this project as a simple procedure. First, the constants in this procedure were determined. These constants were found to be as follows: the material of the skin, a carbon composite weave strengthened with an epoxy; the core of the sandwich construction, a polystyrene foam provided and cut by an outside vendor; and, finally, the basic interior layout of the aircraft.

Next, the variables in this procedure which might have caused problems in the design were determined. These variables were found to be the values of the stresses, forces, etc. that are found through the wing loading analysis. The values which the aerodynamics and stability groups produced were substituted into the appropriate equations and compared to the safe values of the carbon composite weave. If the stresses or shear forces were unacceptable, the other groups were notified in order that the

procedure be started over with a new design, until a legitimate final product was obtained.

4.2 Final Design

Figure 4.1 shows the final interior design of the wing. The absence of a fuselage posed some design limitations, namely placement and access to the electronic and engine components. Thus all the components had to be placed within the wing. In order to simplify construction most of the internal components were placed together in the mid-section of the wing, with access to them through a "trap door" placed on the bottom.

The engines posed a greater problem since they are the heaviest component on the wing and are placed 57 cm from the root creating regions of increased stress concentration. These connections were simplified as much as possible to ease construction, but still maintain structural integrity. The final engine connection attached the duct of the engine directly to the carbon shell by four screws.

4.3 Method of Construction

The wing is a sandwich construction with a carbon fiber composite "face sheet" and an extruded polystyrene "core". This type of construction makes use of the advantages offered by both of the materials used in distributing the load. The "face sheet" or the carbon composite material will carry the majority of the tension and

FIGURE 4.1: INTERIOR DESIGN OF FLYING WING

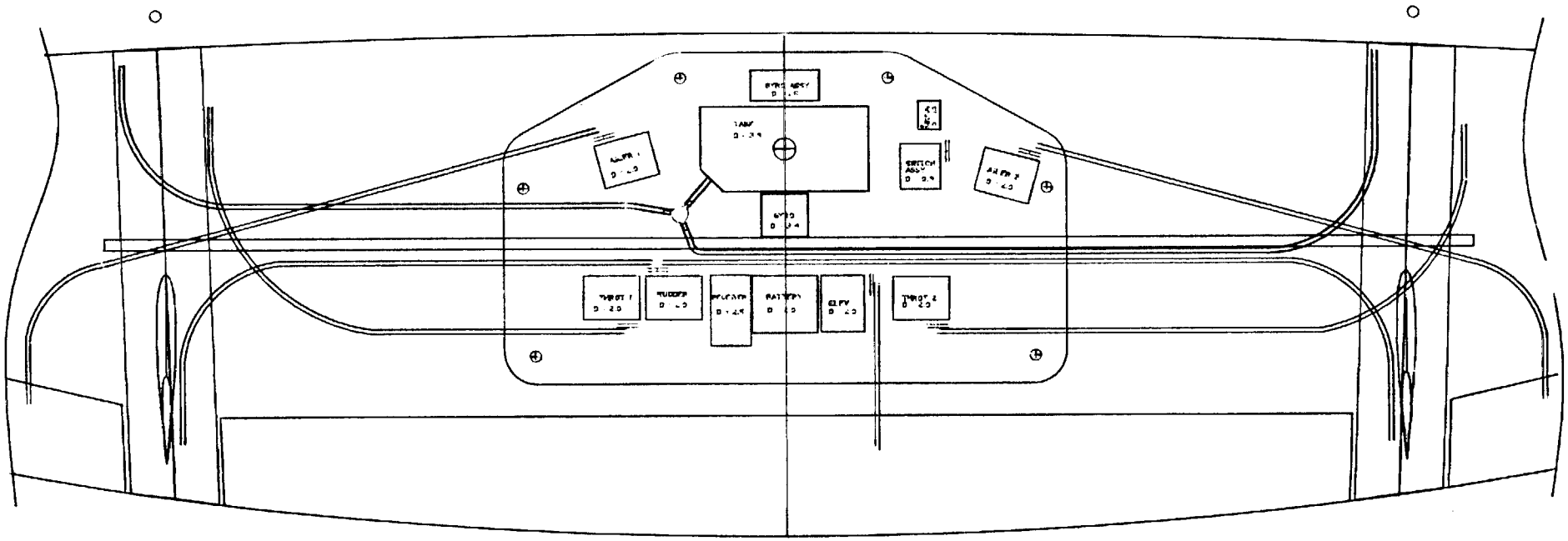

compression loading, while the "core" or extruded polystyrene will carry most of the shear as well as the compression perpendicular to the skin.

In order to construct this type of "material", a process called vacuum bagging was used since it would give the best results. The principle behind vacuum bagging involves placing various layers of carbon/epoxy over the components to be covered. Then an evenly distributed force, of magnitude 4-8 Newtons, is applied across the entire surface of the part. The result is a reduction in the presence of air bubbles as well as removal of excess resin. The presence of excess resin, besides increasing the weight, causes the formation of stress concentration points by inconsistency in strength.

The extruded polystyrene was chosen because it is a rigid foam and therefore helped to attain the desired rigidity. In addition the polystyrene is a foam that is easy to handle. The foam was initially a single oversized piece that needed to be cut and shaped to the desired shape. The airfoil section needed to be hot wired into the planform and the taper had to be appropriately shaped using coarse sandpaper. The engine connections were made through hot wiring the circular sections at a 2 degree outward canter and a 4 degree downward canter. As mentioned previously, the absence of the fuselage forced the placement of the components inside the wing, and thus much of the mid-section had to be hollowed out. A spar was placed in this area in order help regain some of the rigidity that was lost.

Once the wing had been properly shaped, the carbon fiber skin was placed over the foam using the above described vacuum bagging procedure.

4.4 Material Selection

Many important factors had to be considered when selecting the material for the wing. The material had to be within tolerance of the necessary yield and ultimate strength. It had to be stiff, yet have the ability to resist fracturing due to impact during a crash landing. Weight was a main constraint as excessive loads will inhibit the plane's ability to fly. Consequently, the material's weight and density were also a primary concern. The temperature limits also had to be considered in conjunction with the engine. If the engines were to become extremely hot, the material had to be capable of withstanding the heat so as to resist melting or deforming. Finally, the practicality of the material had to be examined. Not only did the material have to be workable with the equipment on hand, but cost and availability were also principal factors.

After much consideration and research, composites were decided to best meet the design requirements. Composites met all of the constraints and offered the largest reduction in weight.

A composite is a combination of two chemically distinct phases whose properties and structural performance is superior to those of the constituents acting independently. A composite is composed of a fiber and a matrix. The fiber supplies the strength and stiffness of the composite and carries most of the load while the matrix supports and transfers the stresses to the fibers. The matrix also protects the fibers from physical damage and the environment. Finally, it provides ductility and toughness to prevent the propagation of cracks. Composites cannot take concentrated loads; therefore, the loads

should be evenly distributed throughout the composite. Composites are only strong in the direction of the fibers; thus, orientation of the fibers is very important. Bidirectional fibers at 90 degrees will withstand vertical and horizontal forces while fibers at 45 degrees are better for torsion. It was determined that the drag forces would be stonger than the forces due to torsion; therefore the 90 degree fiber orientation was chosen. Carbon was the fiber selected (see Table 4.1). Carbon was selected because of its high strength to weight ratio, inherent rigidity, low density, and low cost. Carbon is also relatively easy to mold.

Table 4.1:
Properties of Reinforcing Fibers

TYPE	TENSILE STRENGTH (MPa)	ELASTIC MODULUS (GPa)	DENSITY (kg/m^3)	RELATIVE COST
Boron	3500	380	2600	Highest
Carbon				
High strength	3000	275	1900	Low
High modulus	2000	415	1900	Low
Glass				
E type	3500	73	2480	Lowest
S type	4600	85	2540	Lowest
Kevlar				
29	2800	62	1440	High
49	2800	117	1440	High

Hexel epoxy was chosen as the matrix. Hexel epoxy was chosen primarily for its long pot life. This factor made it easier to work with during construction. Epoxy is a thermoset plastic meaning that once it is cured it is "set" and the reaction cannot be reversed. This made construction a little difficult because no mistakes could be made.

Composites are very strong in tension, but they are relatively weak in compression. For this reason the composite was supported by foam. The foam provided a "cushioning medium" through sandwich construction. Foam did not add much weight and was considerably better in compression. Density was the main consideration when selecting a foam. The higher the density, the better the compression but the heavier it would be. Polystyrene was chosen because it offered an acceptable density and was easy to form.

4.5 Wing Loading Analysis

One of the most important aspects of the structure of the plane was to guarantee minimum bending. If the plane were to bend or twist during flight, the distribution of forces may change greatly which would adversely affect the stability of the plane; therefore it was extremely important to maintain the shape of the platform during flight. In order to verify that the material selected to build the wing would not bend under the loading encountered during flight, an analysis of the stresses at the wing root was performed. The wing was modeled as a cantilever beam since it is symmetric along the root chord. In order to simplify the analysis, the cantilever beam was assumed to have a constant area cross-section unlike the actual model which has an elliptical taper.

Since the wing is of sandwich construction, which consists of two materials, it had to be "transformed" into a single equivalent material. This transformation was

done by creating a ratio of Young's Modulus for the two materials involved, in this case the extruded polystyrene foam and the carbon fiber composite. This ratio then determined an equivalent area for the material. The extruded polystyrene foam was converted mathematically into carbon fiber composite. Below is the ratio of the Moduli of Elasticity of the two materials.

$$n = \frac{E_{foam}}{E_{carbonfiber}} \qquad [4.1]$$

Since this ratio is much less than one it was concluded that the foam can be neglected in the analysis.

The loading was then applied to the beam according to those loads estimated for level cruising. For example, the lift was elliptically distributed along the span. Additionally the drag was uniformly distributed. The weight of the engines and thrust were placed in their appropriate position, according to the numbers obtained from the stability subgroup. The normal stresses were determined using the following equation:

$$\sigma = \frac{P}{A} - \frac{M_x * y}{I_{xx}} + \frac{M_y * x}{I_{yy}} \qquad [4.2]$$

The results are presented in Appendix E. The maximum stresses encountered at the root were calculated to be 23.99 kPa, which is well within the limits the carbon fiber composite strength.

In addition to normal stress, the shear stress was also determined at the root. Once again asymmetric bending was used. The airfoil section was modeled as a closed loop cross-section with a positive shear direction show in Figure 4.2. The results of this analysis are also shown in Appendix E. The shear was estimated to be 108.3 kPa, which is once again well within the limits of the composite material.

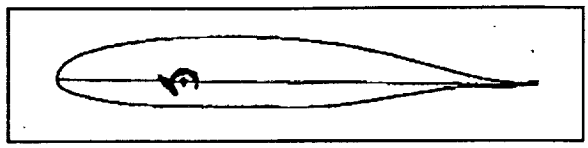

Figure 4.2: Wing Loading

It was realized that the theoretical material strengths were greater than those of the actual values. However, it was believed that the stresses were well within tolerance. The objective was to build a rigid, yet manufacturable wing. Using the suggested method of construction with the chosen materials, it is felt that this goal has been successfully obtained.

CHAPTER FIVE: PROPULSION SYSTEMS

5.1 Introduction

Since the flying wing has no fuselage, it was important to find a method of propulsion which could be easily integrated with the wing. Many important factors needed to be considered when choosing the propulsion system, such as engine type, method of propulsion and total system integration. In addition, the propulsion system was required to produce adequate and controllable thrust to allow for a smooth flight.

5.2 Engine Selection

Two types of engines were considered, electric engines and internal combustion engines. Both of these types of engines have advantages and disadvantages with respect to their usage.

5.2.1 Electric Engines

Electric engines provide clean power. Since no combustion takes place in these systems, noise pollution is minimized. Furthermore, electric engines are easier to maintain when compared to internal combustion engines. Starting an electric engine simply requires a DC power source rather than the fuel, glow plugs and starters needed for internal combustion engines. Hence, electric engines need less time and effort for starting, steady operation and maintenance.

However, the electric engine does have some considerable disadvantages. The most significant is its low thrust to weight ratio (T/W). Batteries, the clean power source for the electric engine, are also its primary detriment. For example, an electric engine which weighs 4.39 N requires three standard 6 Volt batteries weighing 8.01 N. This engine's maximum thrust output is 15.57 N, yielding a max T/W of only 1.26. A comparable internal combustion engine, such as the one chosen for the flying wing, has a max T/W using manufacturer's data of 2.43. A higher T/W allows the flying wing to have better maneuverability in the air, and ensures enough reserve of thrust to maintain flight.

5.2.2 Internal Combustion Engines

In the discussion of the electric engines many of the disadvantages of the internal combustion engines were mentioned. These engines produce plenty of pollution. The testing and operation of these engines must be done in an environment where fresh air can be circulated. Also, two-cycle engines produce tremendous noise pollution, although a muffler attached to the engine will reduce some of the noise pollution. Furthermore, air pollution is created by the exhaust. The unburned castor oil (required for lubrication) spills out from the exhaust, creating further pollution.

The internal combustion engines must be maintained to ensure smooth operation and reduce wear and tear due to the combustion process. Great care is required to assure that no foreign particles enter the combustion chamber. The engine must be cleaned externally, so that debris do not collect on residual oil that lingers on the engine's body.

Some hands on experience is required in the engine's operation. Choosing an optimum fuel/air mixture and controlling the throttle during testing requires careful percision.

The main advantage of the internal combustion engine is its high thrust to weight ratio, since fuel provides more energy per density compared to available batteries. For this reason, the internal combustion engine was chosen for the flying wing. Furthermore, internal combustion engines are widely accepted as the norm in the model airplane industry with the exception of sail planes.

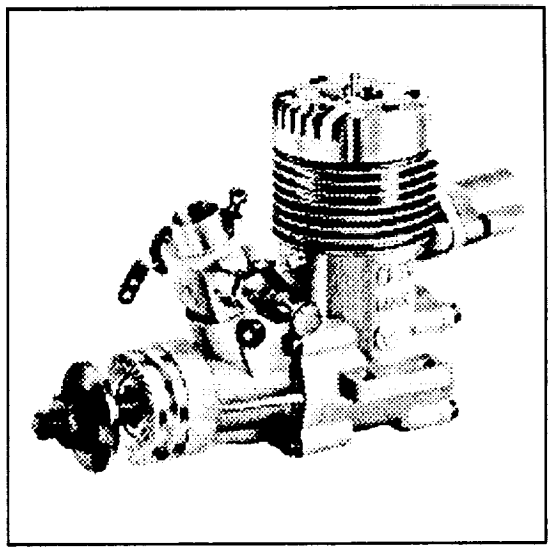

Figure 5.1: 4.07 cc O.S. Engine (O.S. Engines Catalog, 1990)

The flying wing is powered by two 4.07 cc O.S. VF-DF Engines (Figure 5.1). Each engine produces 820.30 Watts at 22,000 rpm and weighs 2.23 N.

5.3 Method of Propulsion

Two main methods of propulsion were considered, propellers and ducted fans. The first method is widely used and accepted in the model airplane industry. The second is a rather new approach and less accepted mode of propulsion.

5.3.1 Propellers

Free propeller driven airplanes are the norm in the model airplane industry. They have been field tested quite extensively and have proven to be reliable. The propulsion system consists of a propeller, an engine and the fuel tank. The propeller can be easily mounted to the driving shaft of the engine. There are no requirements for other major accessories, resulting in reduced weight. Furthermore, the engine is readily accessible, since it is not encased in a duct, in contrast to the ducted fan setup.

There are two major disadvantage with a free propeller setup for the flying wing: propeller wash which interferes with control surfaces, and the large ground clearance required for a large diameter propeller.

Propeller wash is the turbulent thrust produced by the propeller (Figure 5.2). This turbulence affects the control surfaces, namely the vertical stabilizers and the elevator. Since the flying wing is inherently unstable, it is important to keep all control surfaces clear of any disturbances, such as those created by propeller wash.

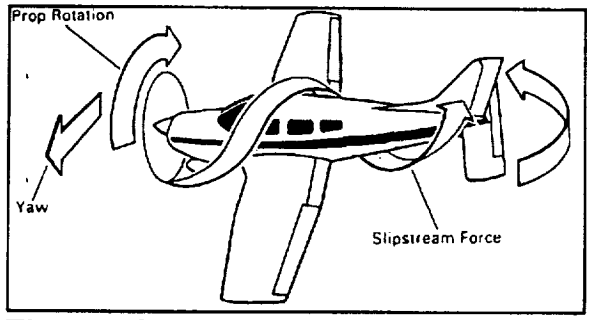

Figure 5.2: Prop Wash on an Airplane (Private Pilot Manual, p. 1-39)

Since propellers have a relatively large diameter compared to the thickness of the flying wing, large landing gear would be required to attain the needed ground clearance. Utilizing large landing gear adds unnecessary drag. However, minimumizing drag was a design goals of the aerodynamics team. Therefore, to maintain stability and aerodynamic integrity, a conclusion was reached not to use a propeller.

5.3.2 Ducted Fan Engines

Although ducted fan engines have a much more complex assembly process than regular propeller engines, their clean aerodynamic shape seemed to fit perfectly in the airfoil, producing enough thrust and yet keeping drag to a minimum.

The ducted fan engine consists of a piston engine enclosed in a cylindrical duct, with a small seven-blade rotor spinning at much higher rpm's than regular propeller engines to produce the same amount of thrust (Figure 5.3). Since the engine is completely enclosed inside the cylindrical housing, it is very hard to assemble the kit or to do any maintenance on the engines. In fact if any problems arise with the engines, the entire kit would have to be removed from the aircraft and then disassembled. The assembly process is rather complicated because extremely tight tolerances have to be kept in order for the fan to work properly. The rotor has to be perfectly balanced, since it rotates at speeds around 22000 rpm. The slightest imbalance would generate undesired vibrations.

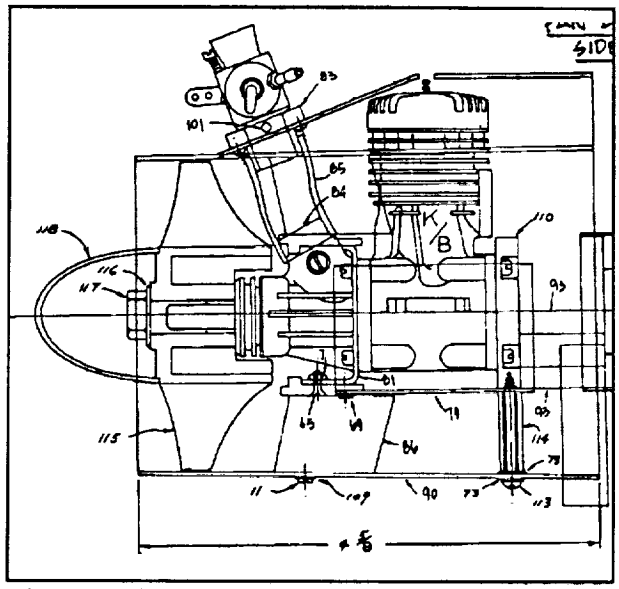

Figure 5.3: Ducted Fan Engine Layout (RK-720 MK III Instructions and Specifications, 1992, page 3)

5.4 Propulsion Systems Configuration

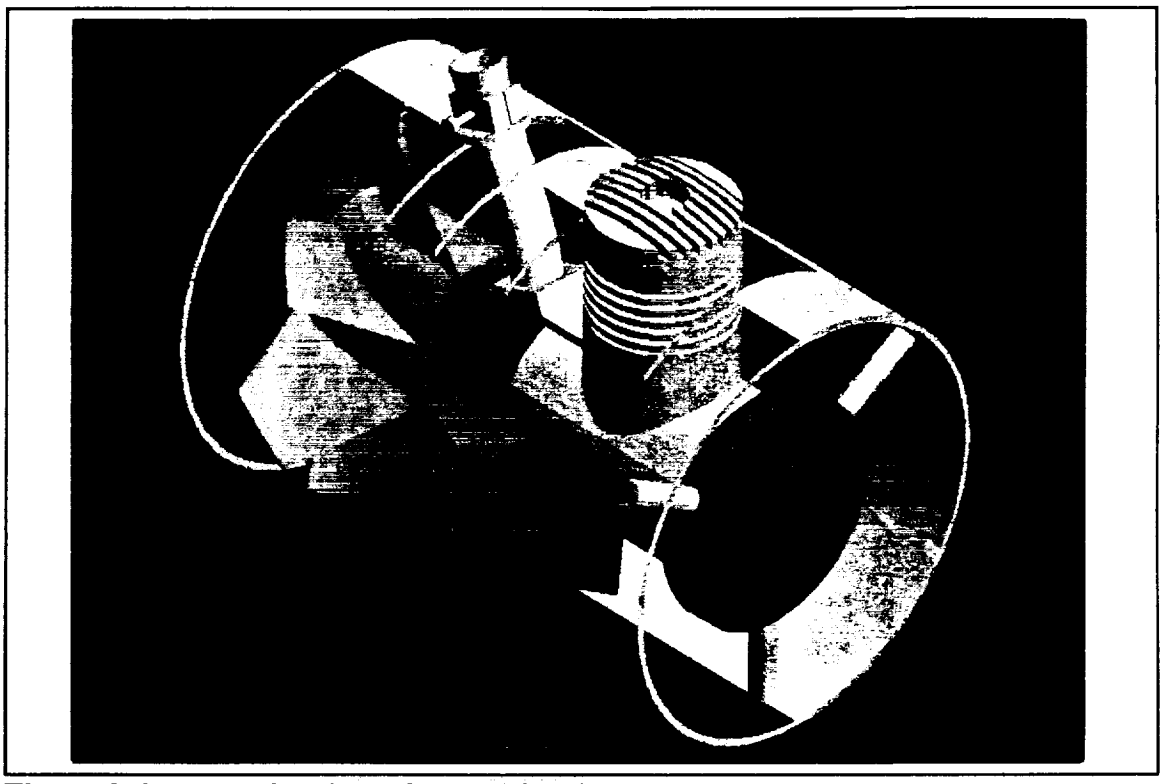

Figure 5.4: Isometric View of Propulsion System Layout

The final configuration of the propulsion system is shown in Figure 5.4. The three dimensional drawing clearly shows the shell, the rotor, the engine, the stator and all the supports. The engine's carburetor and cylinder head protrude from the duct.Each engine assembly as shown, weighs 4.00 N. Both engines receive fuel from a central fuel tank located near the center of gravity of the airplane. The manufacturer's ducted fan test results are shown in Figure 5.5. The operating speed is approximately 22000 RPM, with a resulting thrust of 15.60 N for each engine, which provides more than enough combined thrust to propel the flying wing.

The experimental thrust obtained from strain-gauge measurements is lower than

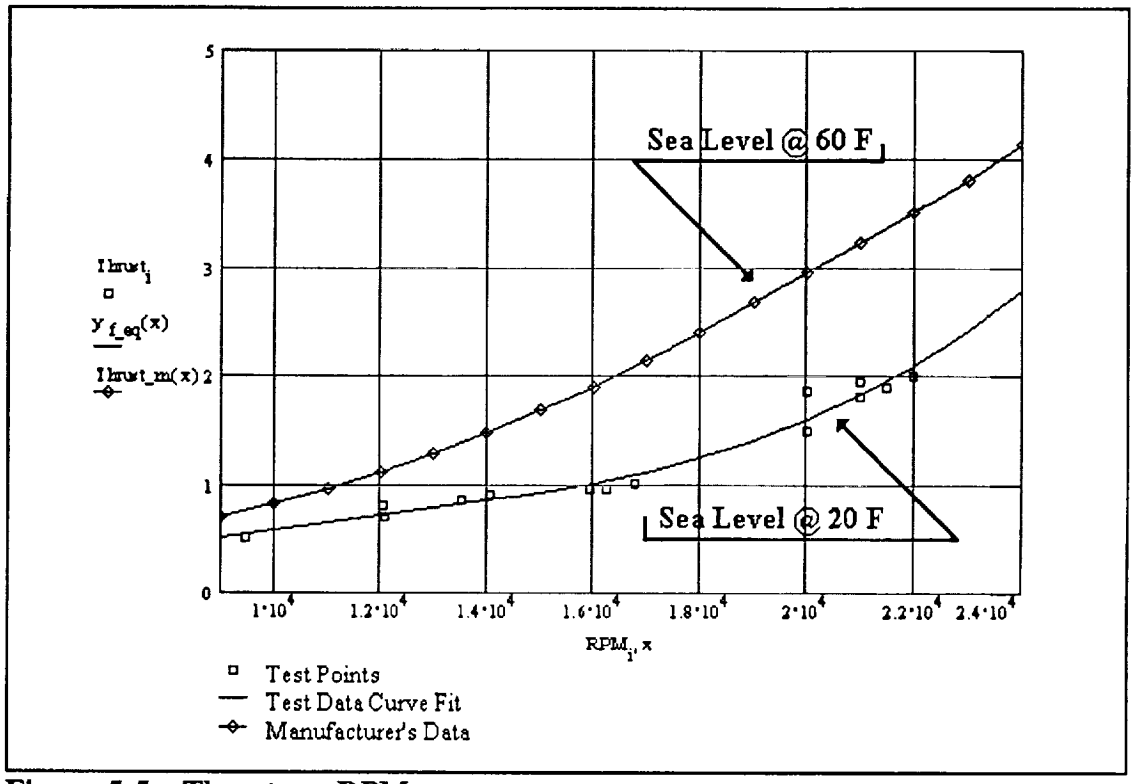

Figure 5.5: Thrust vs. RPM

the manufacturer's results. At 22000 RPM, only 8.9 N of thrust is acquired (Figure 5.5). Even with this lower value, the combined two engine thrust of 17.8 N is more than sufficient to overcome the empirical drag calculated by the aerodynamics sub-group. The ultimate test of the propulsion system will come during the ground and flight testing of the flying wing.

CHAPTER SIX: CONCLUSIONS AND RECOMMENDATIONS

Many engineering difficulties were encountered during the design and construction of the flying wing, *Elang*. After the plane construction was completed, there appeared to be many components and processes which could be further optimized through more research, development and testing. Of course many of these revelations were not obvious to the project team before the actual construction began. The performance of *Elang* depends on the following criteria: overall efficiency of the propulsion system, structural design, material selection, stability, aerodynamic analysis and the overall weight of the plane.

Even though, the propulsion system generated an adequate amount of power, it seemed to generate quite a bit of problems. Since this was original thought as an oblique flying wing two engines were used. However the ability to synchronize the power produced by the engines became more difficult then anticipated. Though the engines preformed fairly well at higher revolutions per minute, at lower revolutions per minute the performance declined. The engines would simply stall. Another point of difficulty was the length of the fuel lines. Each engines draws fuel over a 25 cm line. This appeared to be too much for the small 0.25cc engines to handle. The inability to place a muffler or a tune pipe posed a problem for the design team. For a future design it is recommended to use one large engine or to design an adequate throttle control. A good consideration for throttle control could be one that measures the revolutions per minute

in flight and adjusts for any deviations. The incorporation of tune pipes or mufflers could prove extremely pleasant to the ears.

Stability was of course one of the primary problems with a plane of this type. Finding the center of gravity and designing around that proved extremely difficult. Also, the sizing of the multiple control surfaces was extremely important. The group decided to oversize all control surfaces to account for the inherent instability of an aircraft without a fuselage or horizontal stabilizer. Finally, an airfoil was designed with a positive moment about the aerodynamic center. This characteristic is essential in counteracting the inherent instability of the flying wing.

Aerodynamically, the project group found that the use of computer codes for analysis, although fast and relatively easy, proved to be quite risky. It is recommended that the computer codes used should be verified for proper accuracy and operation prior to using them for design and analysis. Also, not being able to build a prototype model for wind tunnel testing limited the group to purely theoretical aerodynamic analysis.

The aircraft uses three landing gears. One steerable nose gear and two back landing gears. Even though, the design of the landing gears was left for the last minute they seem to preform quit well. The only minor problem was the length and width of the axle which held the front gear. However once the length was shortened and the diameter of the axle increased the problem was solved.

Structurally, *Elang* was very solidly built. The carbon fiber and vacuum bagging technique proved to be very effective. The foam core, although difficult to shape correctly the first time, became quite easy to work with and proved to be the best mold

for the carbon fiber skin. However, the number of carbon composite layers used around the engine, could be reduced from four to maybe two or three layers for simpler construction.

The participation of outside vendors in this project assisted the building team. The use of a 2-D CAD driven hot wire at Foam Technology, saved valuable time and minimized the amount of sanding needed by hand. This produced a more accurate mold which in turn provided a better surface for the carbon to lie on.

Finally, in the area of group dynamics, this project group found that thirteen group members seemed to be too large. It is recommended that, if at all possible, a smaller group size of approximately eight people would be best. This way, communication and coordination of activities will be that much easier.

Overall, the project team was very satisfied with the analysis, design, construction, and performance of *Elang*. The recommendations mentioned above indicate areas in which the project team felt limited. Most of these recommendations were realized through experience and did not come to light until the completion of the aircraft. Further research and development in these areas are encouraged because the possibilities for various design configurations of this type of aircraft are numerous.

REFERENCES

Ault, H.K. & Scott, K.E., WPI CAD LAB IPI Manual of Units, Worcester Polytechnic Institute (Worcester, MA), 1992.

Bohlmann, Eckstrom, Weisshaar, "Static Aeroelastic Tailoring for Oblique Wing Lateral Trim," Journal of Aircraft, vol. 27, no. 6, June 1990.

Etkin, Bernard, Dynamics of Flight: Stabilities and Controls, John Wiley & Sons (New York, NY), 1982.

Flinn, R. & Trojan, P., Engineering Materials and their Applications, Houghton Miffin Company (Boston, MA), 1990.

Hobby Lobby Catalog 20 Summer/Fall 92, Hobby Lobby International (Brentwood,TN), 1992.

Jones, Robert T. & Cohen, Doris, High Speed Wing Theory, Princeton University Press (Princeton, NJ), 1960.

Jones, R.T., "Technical Note: The Flying Wing Supersonic Transport," Aeronautical Journal, March 1991.

Kalpakjian, Serope, Manufacturing Engineering and Technology, Addison Wesley Publishing Company (Reading, MA), 1992.

McEntee, Howard G., The Model Aircraft Handbook, Robert Hale Ltd. (London, England), 1982.

Nelson, Robert C., Flight Stability and Automatic Control, McGraw-Hill Book Company (New York, NY), 1989.

O.S. Engines Catalog, O.S. Engines Mfg. Co. Ltd. (Osaka, Japan), 1990.

RK-720 MK III Instructions and Specifications, Kress Jets,Inc. (Saugerties,NY),1992.

Shevell, Richard S., Fundamentals of Flight, Prentice-Hall Company (Englewood Cliffs, NJ), 1989.

Stinton, Darrol, The Design of the Aeroplane, BSP Professional Books (London, England), 1989.

Tower Hobbies 1993 Catalog, Tower Hobbies (Champaign, IL), 1992.

APPENDIX A

MATHCAD RESULTS FOR STABILITY ANALYSIS

Read Pints from data file (hp33.prn-section points, hp33int.prn-lift, drag, moment)

$i := 0..45 \qquad j := 0..12$

$point := READPRN(points) \qquad LDM := READPRN(ldm)$

$x_{a_i} := point_{i+45,0} \qquad y_{u_i} := point_{i+45,1} \qquad y_{l_i} := point_{45-i,1} \qquad x_{a_{44,0}} := 0.999$

$\alpha_{0_j} := LDM_{j,0} \qquad C_{l_j} := LDM_{j,1} \qquad C_{d_j} := LDM_{j,2} \qquad C_{4_j} := LDM_{j,6} \qquad N \equiv newton$

Angle of Attack α_0	Lift Coefficient C_l	Drag Coefficient C_d	Moment Coefficient about quater chord C_4
-2	-0.196	0.0015	0.0231
-1	-0.074	0.0009	0.0211
0	0.048	0.0005	0.0191
1	0.17	0.0003	0.017
2	0.292	0.0003	0.0148
3	0.414	0.0005	0.0125
4	0.536	0.0009	0.0106
5	0.657	0.0015	0.0085
6	0.779	0.0022	0.0066
7	0.9	0.0032	0.0048
8	1.021	0.0044	0.0031
9	1.141	0.0057	0.0016
10	1.261	0.0073	0.0003

Spline fit the lift, drag and moment curves

$vC_L := cspline(\alpha_0, C_l) \qquad C_L(\alpha) := interp(vC_L, \alpha_0, C_l, \alpha)$

$vC_D := cspline(\alpha_0, C_d) \qquad C_D(\alpha) := interp(vC_D, \alpha_0, C_d, \alpha)$

$vC_{m4} := cspline(\alpha_0, C_d) \qquad C_{m4}(\alpha) := interp(vC_{m4}, \alpha_0, C_4, \alpha)$

$\alpha := -2, -1.9..10$

C_L vs. α

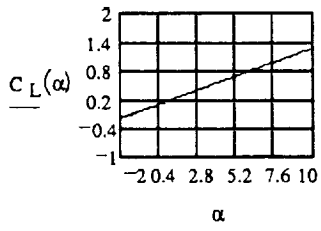

C_D vs. C_L

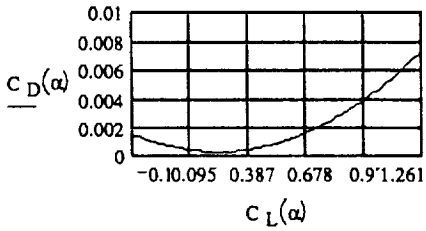

C_{m4} vs. α

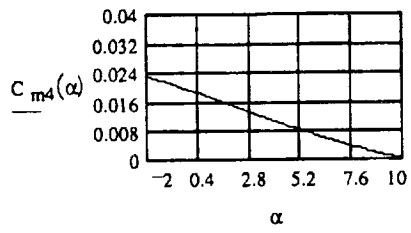

C_L/C_D vs. α

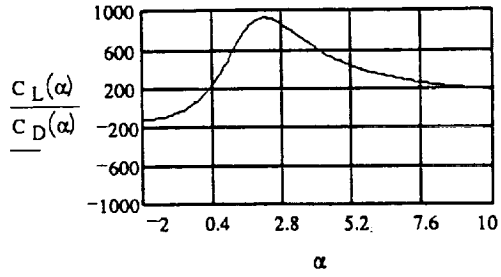

Design Parameters

$w_w := 16 \cdot N$ Weight wing

$w_{ee} := 5.719 \cdot N$ Weight engine empty

$w_{ef} := 9.578 \cdot N$ Weight engine with fuel

$x_{wcg} := 0.209 \cdot m$ Wing x center of gravity

$y_{wcg} := 0.00561 \cdot m$ Wing y center of gravity

$v := 15.0 \cdot \frac{m}{sec}$ Cruise velocity

$T_e := \frac{50}{30} \cdot N$ Cruise thrust

$q := \frac{1}{2} \cdot \rho \cdot v^2$ Dynamic pressure

$q = 137.813 \cdot Pa$

$S := 0.893 \cdot m^2$ Wing surface area

$y_{cp} := 0 \cdot m$ $qs := q \cdot S$ $w_e := w_{ee}$

$\beta := 0 \cdot deg$ Sweep Angle

$\Gamma := 0 \cdot deg$ Engine pitch angle

$\rho := 1.225 \cdot \frac{kg}{m^3}$ Sea level density

$cord := 0.455 \cdot m$ Cord lenght

$\alpha_n := 4$ Cruise angle

$thick_{max} := \left(\max\left(y_u\right) + \left|\min\left(y_l\right)\right|\right) \cdot cord$

$thick_{max} = 0.067 \cdot m$ Airfoil thicknes

Cruise conditions

$C_L(\alpha_n) = 0.536$

$C_D(\alpha_n) = 8.911 \cdot 10^{-4}$

$C_{m4}(\alpha_n) = 0.011$

$AR := 7$

Spline airfoil coordinates

$vY_u := cspline\left(x_a \cdot cord, y_u \cdot cord\right)$

$vY_l := cspline\left(x_a \cdot cord, y_l \cdot cord\right)$

$Y_u(x) := interp\left(vY_u, x_a \cdot cord, y_u \cdot cord, x\right)$

$Y_l(x) := interp\left(vY_l, x_a \cdot cord, y_l \cdot cord, x\right)$

Aerodynamic center, and C_{Mac}

$$X_{cp}(\alpha) := \left(\frac{1}{4} - \frac{C_{m4}(\alpha)}{C_L(\alpha)}\right) \cdot cord \qquad x_{ac}(\alpha) := \left[\left(\frac{d}{d\alpha} C_L(\alpha)\right) \cdot X_{cp}(\alpha) + C_L(\alpha) \cdot \frac{d}{d\alpha} X_{cp}(\alpha)\right] \cdot \frac{1}{\frac{d}{d\alpha} C_L(\alpha)}$$

$$C_{mac}(\alpha) := \frac{C_L(\alpha)}{cord} \cdot \left(x_{ac}(\alpha) - X_{cp}(\alpha)\right)$$

$\alpha := -2, -1.5 .. 10$

X_{ac} vs. α

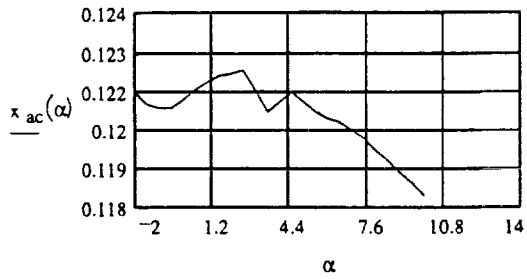

C_{mac} vs. α

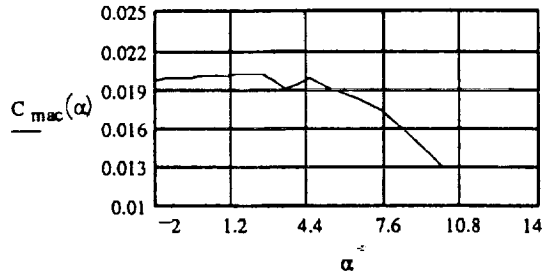

$C_{mac}(\alpha) := C_{mac}(\alpha)\cdot\cos(\beta)$

$C_{mac}(\alpha_n) = 0.019$

$M_{ac}(\alpha) := C_{mac}(\alpha)\cdot qs\cdot cord$

$M_{ac}(\alpha_n) = 1.088\cdot m\cdot N$

$C_{Lu}(\alpha) := C_L(\alpha)\cdot\cos(\alpha\cdot deg)$

$C_{Lb}(\alpha) := C_L(\alpha)\cdot\sin(\alpha\cdot deg)\cdot\cos(\beta)$

$C_{Db}(\alpha) := C_D(\alpha)\cdot\cos(\alpha\cdot deg)\cdot\cos(\beta)$

$C_{Dd}(\alpha) := -C_D(\alpha)\cdot\sin(\alpha\cdot deg)$

$L_u(\alpha) := C_{Lu}(\alpha)\cdot qs$

$L_b(\alpha) := C_{Lb}(\alpha)\cdot qs$

$D_b(\alpha) := C_{Db}(\alpha)\cdot qs$

$D_d(\alpha) := C_{Dd}(\alpha)\cdot qs$

$L_u(\alpha_n) = 65.769\cdot N$

$L_b(\alpha_n) = 4.599\cdot N$

$D_d(\alpha_n) = -0.008\cdot N$

$D_b(\alpha_n) = 0.109\cdot N$

$x_L(\alpha) := x_{ac}(\alpha)$

$T_{e20} := T_e\cdot\cos(\beta)$

$T_{e20} = 1.667\cdot N$

$T_f := T_{e20}\cdot\cos(\Gamma)$

$T_d := T_{e20}\cdot\sin(\Gamma)$

$T_f = 1.667\cdot N$

$T_d = 0\cdot N$

Extra mass estimation

$w_{mass} := 0.5\cdot kg\cdot g \qquad x_{mass} := 0.05\cdot m \qquad y_{mass} := y_{wcg}$

$$x_{cg}(x_{ecg}) := \frac{x_{ecg}\cdot(2\cdot w_e) + x_{wcg}\cdot w_w + x_{mass}\cdot w_{mass}}{(2\cdot w_e + w_w + w_{mass})}$$

$$y_{cg}(y_{ecg}) := \frac{y_{ecg}\cdot(2\cdot w_e) + y_{wcg}\cdot w_w + y_{mass}\cdot w_{mass}}{(2\cdot w_e + w_w + w_{mass})}$$

$$\begin{aligned} M(x_{ecg}, y_{ecg}, \alpha) := {} & M_{ac}(\alpha) \ldots \\ & + L_u(\alpha)\cdot(x_{cg}(x_{ecg}) - x_L(\alpha)) \ldots \\ & + -L_b(\alpha)\cdot(y_{cg}(y_{ecg}) - y_{cp}) \ldots \\ & + D_d(\alpha)\cdot(x_{cg}(x_{ecg}) - x_L(\alpha)) \ldots \\ & + -D_b(\alpha)\cdot(y_{cg}(y_{ecg}) - y_{cp}) \end{aligned}$$

$$C_M(x_{ecg}, y_{ecg}, \alpha) := C_{mac}(\alpha) \ldots + C_{Lu}(\alpha)\cdot\left(x_{cg}(x_{ecg}) - x_L(\alpha)\right)\cdot\frac{1}{cord} \ldots + -C_{Lb}(\alpha)\cdot\left(y_{cg}(y_{ecg}) - y_{cp}\right)\cdot\frac{1}{cord} \ldots + C_{Dd}(\alpha)\cdot\left(x_{cg}(x_{ecg}) - x_L(\alpha)\right)\cdot\frac{1}{cord} \ldots + -C_{Db}(\alpha)\cdot\left(y_{cg}(y_{ecg}) - y_{cp}\right)\cdot\frac{1}{cord}$$

Solve The above equations in order to detremine the position of the engines

$\alpha_n = 4$ $\quad y_{ecg} := y_{wcg}$ $\quad x_{ecg} := 0\cdot m$ $\quad x_{ecg} := root\left(M(x_{ecg}, y_{ecg}, \alpha_n), x_{ecg}\right)$

$x := -0.1\cdot m, 0\cdot m .. cord$

Moment About the Center of Gravity

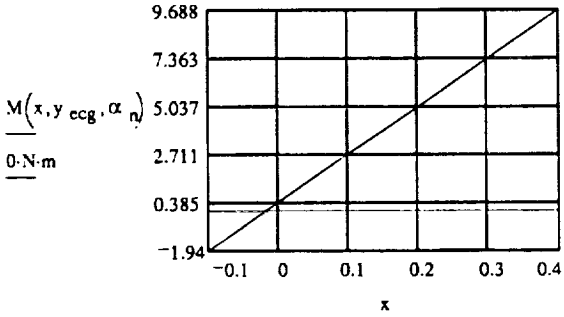

Solution:

$w_e = 5.719\cdot N$

$x_{ecg} = -0.01657\cdot m$ $\quad x_{cg}(x_{ecg}) = 0.10512\cdot m$

$y_{ecg} = 0.00561\cdot m$ $\quad y_{cg}(y_{ecg}) = 0.00561\cdot m$

$w_{mass} = 4.903\cdot N$

$x_{mass} = 0.05\cdot m$ $\quad y_{mass} = 0.006\cdot m$

$\alpha := -2, -1.5 .. 10$

Static Stability: Coefficent of Moment About the Center of Gravity

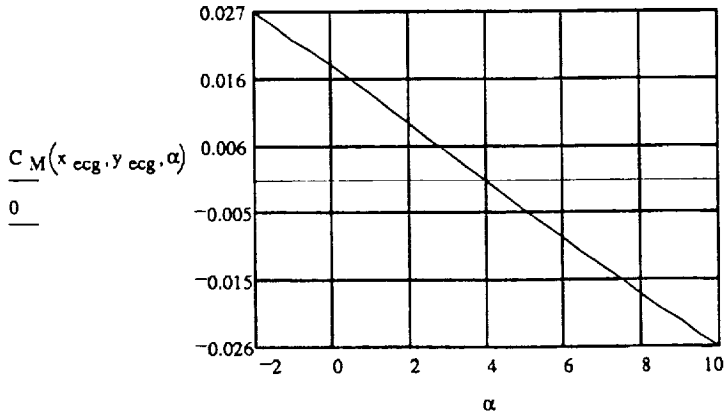

$b := y_{ecg} - \Gamma \cdot x_{ecg}$ $y(x) := \Gamma \cdot x + b$ $yc(x) := 0.00 \cdot x$ $xx := 0 \cdot m, 0.01 \cdot m .. cord$

$x1 := 0 \cdot m, 0.05 \cdot m .. cord$ $x_j := x_{ecg} - 0.02 \cdot m$ $x_f := x_{ecg} + 0.02 \cdot m$ $x := x_j, x_j + 0.01 \cdot m .. x_f$

Side View

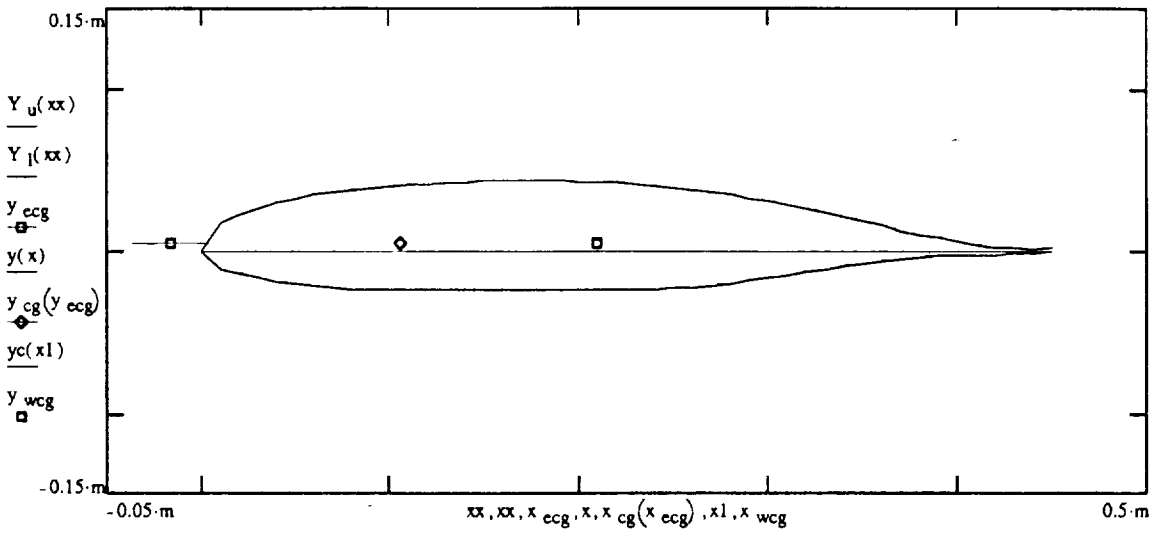

$span := 1.25 \cdot m$ $xx := 0.57 \cdot m$ $x := -1.25 \cdot m, -1.20 \cdot m .. 1.25 \cdot m$

$$y_{eu}(x) := \sqrt{\left(\frac{cord}{4}\right)^2 \cdot \left(1 - \frac{x^2}{span^2}\right)} \qquad y_{el}(x) := -\sqrt{\left(\frac{3 \cdot cord}{4}\right)^2 \cdot \left(1 - \frac{x^2}{span^2}\right)}$$

Top View

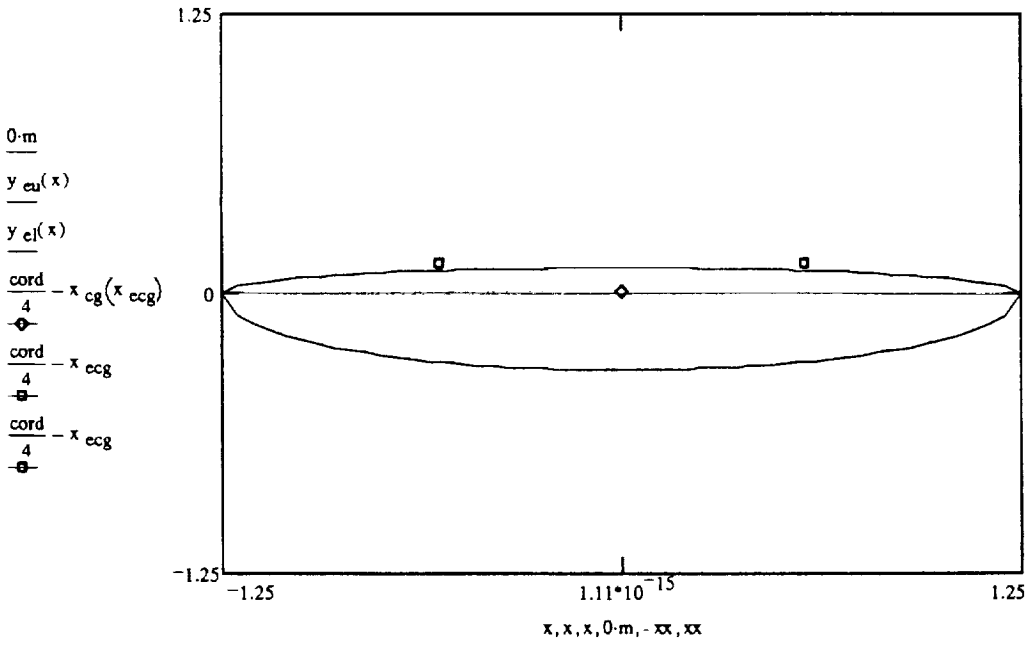

Spline fit the lift, drag and moment curves for the control surfaces

$vC_{Ldef} := cspline(\alpha_{D0}, C_{Ldef0})$ $\quad C_{Ldef}(\alpha) := interp(vC_{Ldef}, \alpha_{D0}, C_{Ldef0}, \alpha)$

$vC_{Ddef} := cspline(\alpha_{D0}, C_{Ddef0})$ $\quad C_{Ddef}(\alpha) := interp(vC_{Ddef}, \alpha_{D0}, C_{Ddef0}, \alpha)$

$vC_{C4def} := cspline(\alpha_{D0}, C_{Ddef0})$ $\quad C_{C4def}(\alpha) := interp(vC_{C4def}, \alpha_{D0}, C_{C4def0}, \alpha)$

$\alpha_D := -30..30$

C_L vs. α

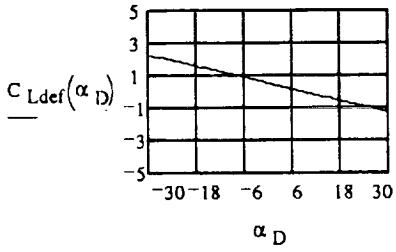

C_D vs. C_L

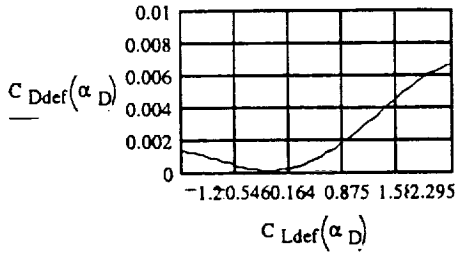

C_{m4} vs. α

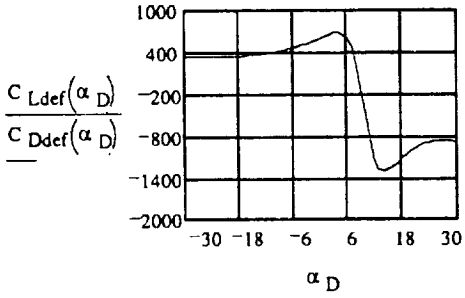

C_L/C_D vs. α

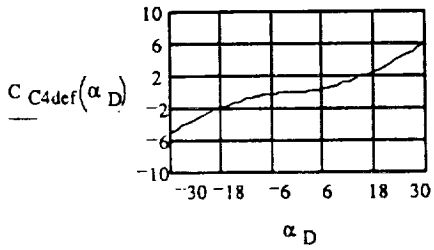

Elevator Analysis

$x_{Ldef} := \frac{cord}{4}$ $\quad x_{Ldef} = 0.114 \cdot m$ $\quad \alpha_n = 4$ $\quad x_L := x_L(\alpha_n)$

$s_{def} := 0.02 \cdot S$ $\quad s_{def} = 0.018 \cdot m^2$ $\quad width := \frac{s_{def}}{.18 \cdot cord}$ $\quad width = 0.218 \cdot m$

$qs_{def} := q \cdot s_{def}$ $\quad qs_{def} = 2.461 \cdot N$ $\quad qs_w := qs - qs_{def}$ $\quad qs_w = 120.605 \cdot N$

$C_{Ludef}(\alpha_D) := C_{Ldef}(\alpha_D) \cdot \cos(\alpha_D \cdot deg)$ $\quad L_{udef}(\alpha_D) := C_{Ludef}(\alpha_D) \cdot qs_{def}$

$C_{Lbdef}(\alpha_D) := C_{Ldef}(\alpha_D) \cdot \sin(\alpha_D \cdot deg) \cdot \cos(\beta)$ $\quad L_{bdef}(\alpha_D) := C_{Lbdef}(\alpha_D) \cdot qs_{def}$

$C_{Dbdef}(\alpha_D) := C_{Ddef}(\alpha_D) \cdot \cos(\alpha_D \cdot deg) \cdot \cos(\beta)$ $\quad D_{bdef}(\alpha_D) := C_{Dbdef}(\alpha_D) \cdot qs_{def}$

$C_{Dddef}(\alpha_D) := -C_{Ddef}(\alpha_D) \cdot \sin(\alpha_D \cdot deg)$ $\quad D_{ddef}(\alpha_D) := -C_{Dddef}(\alpha_D) \cdot qs_{def}$

$M_{C4def}(\alpha_D) := C_{C4def}(\alpha_D) \cdot qs_{def} \cdot cord \cdot \cos(\beta)$

Control Surfaces

Read Pints from data file (flap33.prn-lift, drag, moment)

$j := 0..32$

$LDM_d := READPRN(flap)$

$\alpha_{D0_j} := LDM_{d_{j,0}} \quad C_{Ldef0_j} := LDM_{d_{j,1}} \quad C_{Ddef0_j} := LDM_{d_{j,2}} \quad C_{C4def0_j} := LDM_{d_{j,6}}$

Angle of Attack α_{D0}	Lift Coefficient C_{Ldef0}	Drag Coefficient C_{Ddef0}	Moment Coefficient about quater chord C_{C4def0}
-30	2.295	0.00664	-5.021
-26	2.074	0.00624	-3.804
-22	1.847	0.00557	-2.757
-18	1.615	0.00472	-1.857
-16	1.498	0.00426	-1.464
-12	1.261	0.0033	-0.801
-10	1.141	0.00283	-0.552
-9	1.081	0.0026	-0.446
-8	1.021	0.00238	-0.35
-7	0.961	0.00216	-0.264
-6	0.9	0.00195	-0.19
-5	0.84	0.00175	-0.133
-4	0.779	0.00155	-0.085
-3	0.718	0.00137	-0.052
-2	0.658	0.0012	-0.03
-1	0.597	0.00104	-0.015
0	0.536	0.00089	0.011
1	0.475	0.00076	0.05
2	0.414	0.00063	0.103
3	0.353	0.00052	0.167
4	0.292	0.00043	0.245
5	0.231	0.00035	0.334
6	0.169	0.00028	0.437
7	0.109	0.00023	0.55
8	0.048	0.00019	0.676
9	-0.013	0.00017	0.814
10	-0.074	0.00016	0.965
12	-0.196	0.00017	1.302
16	-0.437	0.00035	2.107
18	-0.557	0.0005	2.571
22	-0.794	0.00085	3.611
26	-1.027	0.00118	4.783
30	-1.256	0.00138	6.068

$\alpha_{Dn} := 4$

$L_u(\alpha_D) := C_{Lu}(\alpha_D) \cdot qs_w \qquad L_b(\alpha_D) := C_{Lb}(\alpha_D) \cdot qs_w$

$D_d(\alpha_D) := C_{Dd}(\alpha_D) \cdot qs_w \qquad D_b(\alpha_D) := C_{Db}(\alpha_D) \cdot qs_w$

$M_{ac}(\alpha_D) := C_{mac}(\alpha_D) \cdot qs_w \cdot \cos(\beta) \cdot cord$

$$\begin{aligned} M_{def}(x_{ecg}, y_{ecg}, \alpha_D, \alpha) := {} & M_{ac}(\alpha) \ldots \\ & + L_u(\alpha) \cdot (x_{cg}(x_{ecg}) - x_L) \ldots \\ & + -L_b(\alpha) \cdot (y_{cg}(y_{ecg}) - y_{cp}) \ldots \\ & + D_d(\alpha) \cdot (x_{cg}(x_{ecg}) - x_L) \ldots \\ & + -D_b(\alpha) \cdot (y_{cg}(y_{ecg}) - y_{cp}) \ldots \\ & + M_{C4def}(\alpha_D) \ldots \\ & + L_{udef}(\alpha_D) \cdot (x_{cg}(x_{ecg}) - x_{Ldef}) \ldots \\ & + -L_{bdef}(\alpha_D) \cdot (y_{cg}(y_{ecg}) - y_{cp}) \ldots \\ & + D_{ddef}(\alpha_D) \cdot (x_{cg}(x_{ecg}) - x_{Ldef}) \ldots \\ & + -D_{bdef}(\alpha_D) \cdot (y_{cg}(y_{ecg}) - y_{cp}) \end{aligned}$$

Moment About the Center of Gravity (For Control Surface)

$M_{def}(x_{ecg}, y_{ecg}, \alpha_D, \alpha_n)$

$0 \cdot N \cdot m$

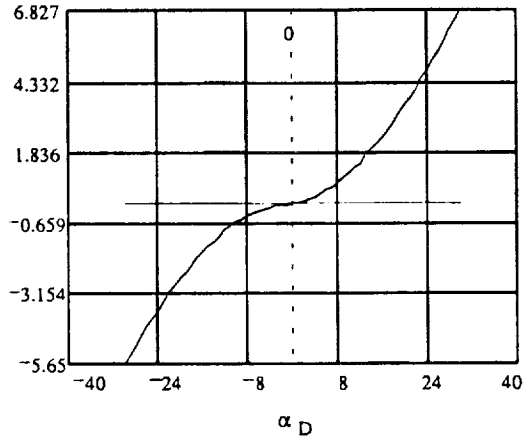

$w_e = 5.719 \cdot N$

$x_{ecg} = -0.017 \cdot m \quad y_{ecg} = 0.006 \cdot m$

$y_{cg}(y_{ecg}) = 0.006 \cdot m$

$x_{cg}(x_{ecg}) = 0.105 \cdot m$

$s_{def} = 0.018 \cdot m^2$

$width = 0.218 \cdot m$

$I\_shell_{zz} := 0.03639 \cdot kg \cdot m^2 \qquad I_{zz} := I\_shell_{zz} + 2 \cdot \frac{w_e}{g} \cdot \left(x_{ecg}^2 + y_{ecg}^2\right) + \frac{w_{mass}}{g} \cdot \left(x_{mass}^2 + y_{mass}^2\right)$

$I_{zz} = 0.038 \cdot kg \cdot m^2 \qquad angular\ \alpha a(\alpha_D, \alpha) := \frac{M_{def}(x_{ecg}, y_{ecg}, \alpha_D, \alpha)}{I_{zz}}$

Angular Acceleration

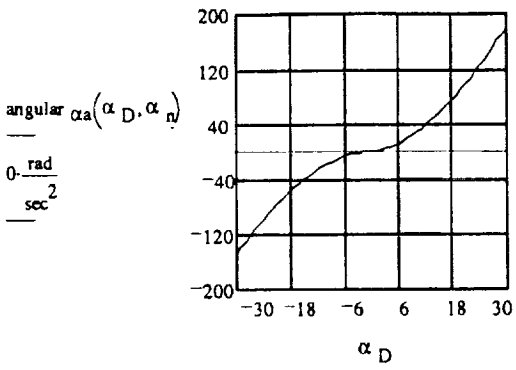

Angular Acceleration

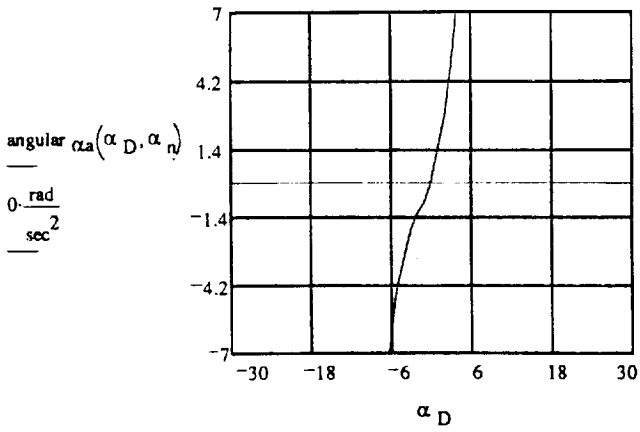

Aileron Analysis

$s_{def} := 0.02 \cdot S$ $s_{def} = 0.018 \cdot m^2$ $width := \frac{s_{def}}{0.18 \cdot cord}$ $width = 0.218 \cdot m$

$qs_{def} := q \cdot s_{def}$ $qs_w := qs - qs_{def}$ $qs_w = 120.605 \cdot N$

$C_{Ludef}(\alpha_D) := C_{Ldef}(\alpha_D) \cdot \cos(\alpha_D \cdot deg)$ $L_{udef}(\alpha_D) := C_{Ludef}(\alpha_D) \cdot qs_{def}$

$C_{Dddef}(\alpha_D) := -C_{Ddef}(\alpha_D) \cdot \sin(\alpha_D \cdot deg)$ $D_{ddef}(\alpha_D) := -C_{Dddef}(\alpha_D) \cdot qs_{def}$

$L_u(\alpha_D) := C_{Lu}(\alpha_D) \cdot qs_w$

$L_{ldef}(\alpha_D) := L_{udef}(\alpha_D)$
$L_{rdef}(\alpha_D) := L_{udef}(\alpha_D)$

$D_{ldef}(\alpha_D) := D_{ddef}(\alpha_D)$
$D_{rdef}(\alpha_D) := D_{ddef}(\alpha_D)$

$x_{ecg} := 0 \cdot m$ $y_{ecg} := 0 \cdot m$

$I_{xx} := 0.621611 \cdot kg \cdot m^2$

$z_{al} := 1 \cdot m$ $z_{ar} := z_{al}$

$M_{rdef}(\alpha_D) := L_{ldef}(\alpha_D + 30) \cdot z_{al} \ldots$
$+ -\left(L_{rdef}(30 - \alpha_D) \cdot z_{ar}\right) \ldots$
$+ -\left(D_{ldef}(\alpha_D + 30) \cdot z_{al}\right) \ldots$
$+ D_{rdef}(30 - \alpha_D) \cdot z_{ar}$

$angular_{\alpha a}(\alpha_D) := \frac{M_{rdef}(\alpha_D)}{I_{xx}}$

Moment About the Center of Gravity (For Control Surface)

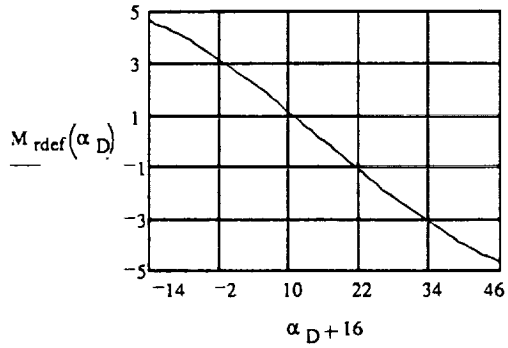

Angular Acceleration

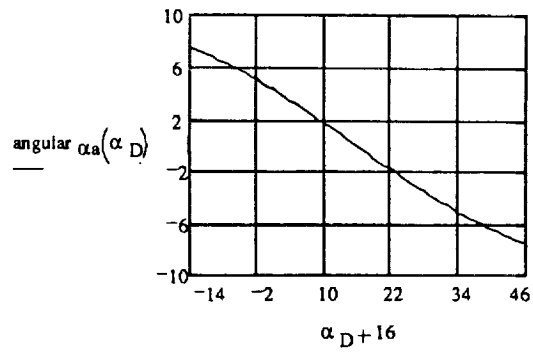

Rudder Analysis

Read Pints from data file (sd8020.prn-lift, drag, moment)

$j := 16..32$

$LDM_r := READPRN(rudder)$

$\alpha_{r1_{j-16}} := LDM_{r_{j,0}}$ $c_{Lr_{j-16}} := LDM_{d_{j-16,1}}$ $c_{Dr_{j-16}} := LDM_{d_{j,2}}$ $c_{C4r_{j-16}} := LDM_{d_{j,6}}$

Angle of Attack

$$\alpha_{r1} = \begin{bmatrix} 0 \\ 1 \\ 2 \\ 3 \\ 4 \\ 5 \\ 6 \\ 7 \\ 8 \\ 9 \\ 10 \\ 12 \\ 16 \\ 18 \\ 22 \\ 26 \\ 30 \end{bmatrix}$$

Lift Coefficient

$$c_{Lr} = \begin{bmatrix} 2.295 \\ 2.074 \\ 1.847 \\ 1.615 \\ 1.498 \\ 1.261 \\ 1.141 \\ 1.081 \\ 1.021 \\ 0.961 \\ 0.9 \\ 0.84 \\ 0.779 \\ 0.718 \\ 0.658 \\ 0.597 \\ 0.536 \end{bmatrix}$$

Drag Coefficient

$$c_{Dr} = \begin{bmatrix} 0.00089 \\ 0.00076 \\ 0.00063 \\ 0.00052 \\ 0.00043 \\ 0.00035 \\ 0.00028 \\ 0.00023 \\ 0.00019 \\ 0.00017 \\ 0.00016 \\ 0.00017 \\ 0.00035 \\ 0.0005 \\ 0.00085 \\ 0.00118 \\ 0.00138 \end{bmatrix}$$

Moment Coefficient about quater chord

$$c_{C4r} = \begin{bmatrix} 0.011 \\ 0.05 \\ 0.103 \\ 0.167 \\ 0.245 \\ 0.334 \\ 0.437 \\ 0.55 \\ 0.676 \\ 0.814 \\ 0.965 \\ 1.302 \\ 2.107 \\ 2.571 \\ 3.611 \\ 4.783 \\ 6.068 \end{bmatrix}$$

$h := 0..16$

$\alpha_{r0_h} := -\alpha_{r1_{(16-h)}}$ $\alpha_{r0_{(16+h)}} := \alpha_{r1_{(h)}}$ $C_{Lr0_h} := -c_{Lr_{(16-h)}}$ $C_{C4r0_h} := c_{C4r_{(16-h)}}$ $C_{C4r0_{(16+h)}} := c_{C4r_h}$

$C_{Dr0_h} := c_{Dr_{(16-h)}}$ $C_{Dr0_{(16+h)}} := c_{Dr_h}$ $C_{Lr0_{(16+h)}} := c_{Lr_h}$

Spline fit the lift, drag and moment curves for rudder control

$vC_{Lr} := cspline(\alpha_{r0}, C_{Lr0})$ $\quad C_{Lr}(\alpha) := interp(vC_{Lr}, \alpha_{r0}, C_{Lr0}, \alpha)$

$vC_{Dr} := cspline(\alpha_{r0}, C_{Dr0})$ $\quad C_{Dr}(\alpha) := interp(vC_{Dr}, \alpha_{r0}, C_{Dr0}, \alpha)$

$vC_{C4r} := cspline(\alpha_{r0}, C_{Dr0})$ $\quad C_{C4r}(\alpha) := interp(vC_{C4def}, \alpha_{r0}, C_{C4r0}, \alpha)$

$cord_r := 0.15 \cdot m$

$S_r := 0.02 \cdot S$ $\quad qs_r := q \cdot S_r$ $\quad Lenght_r := 0.3 \cdot cord_r$ $\quad width_r := \frac{S_r}{cord_r}$ $\quad S_{rs} := width_r \cdot Lenght_r$

$S_r = 0.018 \cdot m^2$ $\quad qs_r = 2.461 \cdot N$ $\quad Lenght_r = 0.045 \cdot m$ $\quad width_r = 0.119 \cdot m$ $\quad S_{rs} = 0.005 \cdot m^2$

$L_r(\alpha_r) := C_{Lr}(\alpha_r) \cdot qs_r$ $\quad L_{rz}(\alpha_r) := L_r(\alpha_r) \cdot \cos(\beta)$ $\quad L_{rx}(\alpha_r) := L_r(\alpha_r) \cdot \sin(\beta)$

$D_r(\alpha_r) := C_{Dr}(\alpha_r) \cdot qs_r$ $\quad D_{rz}(\alpha_r) := D_r(\alpha_r) \cdot \sin(\beta)$ $\quad D_{rx}(\alpha_r) := -D_r(\alpha_r) \cdot \cos(\beta)$

$x_{Lr} := \frac{cord_r}{4}$ $\quad x_{Lrz} := x_{Lr} \cdot \sin(\beta)$ $\quad x_{Lrx} := x_{Lr} \cdot \cos(\beta)$

$z_{lr} := 0.57 \cdot m$ $\quad x_{lr} := 0.1 \cdot m$

$z_{rr} := 0.57 \cdot m$ $\quad x_{rr} := 0.1 \cdot m$

$M_{lr}(\alpha_r) := (L_{rx}(\alpha_r) + D_{rx}(\alpha_r)) \cdot (z_{lr} - x_{Lrz}) - (L_{rz}(\alpha_r) + D_{rz}(\alpha_r)) \cdot (x_{lr} + x_{Lrx})$

$M_{rr}(\alpha_r) := -[(L_{rx}(\alpha_r) + D_{rx}(\alpha_r)) \cdot (z_{rr} + x_{Lrz})] - (L_{rz}(\alpha_r) + D_{rz}(\alpha_r)) \cdot (x_{rr} + x_{Lrx})$

$M_r(\alpha_r) := M_{lr}(\alpha_r) + M_{rr}(\alpha_r)$

$\alpha_r := -30..30$

Moment About the Center of Gravity (For Control Surface)

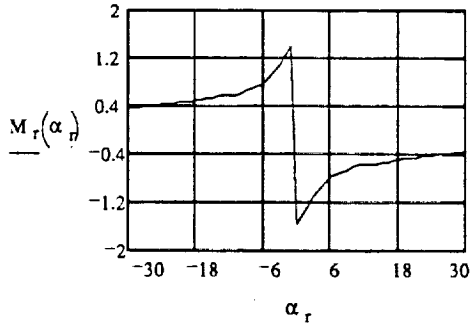

$width_r = 0.119 \cdot m$

$Lenght_r = 0.045 \cdot m$

$S_{rs} = 0.005 \cdot m^2$

$I_{yy} := 0.656673 \cdot kg \cdot m^2$ $\quad angular_{\alpha r}(\alpha_r) := \frac{M_r(\alpha_r)}{I_{yy}}$

Angular Acceleration

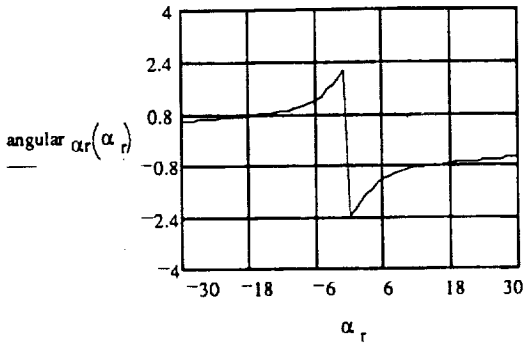

APPENDIX B

COORDINATES AND DATA FOR HPRS 33

AIRFOIL SECTION

Coordinates for HPRS 33 Airfoil Section

X	Y(upper)	Y(lower)
0.00000	0.00000	0.00000
0.00182	0.01182	-0.00860
0.00455	0.01850	-0.01275
0.01136	0.02790	-0.01812
0.02273	0.03786	-0.02377
0.03409	0.04522	-0.02818
0.04545	0.05091	-0.03152
0.06818	0.05965	-0.03717
0.09091	0.06645	-0.04151
0.11364	0.07190	-0.04493
0.13636	0.07648	-0.04792
0.15909	0.08044	-0.05034
0.18182	0.08372	-0.05134
0.22727	0.08889	-0.05234
0.27273	0.09245	-0.05234
0.31818	0.09463	-0.05234
0.36364	0.09545	-0.05234
0.42209	0.09505	-0.05234
0.46755	0.09335	-0.05234
0.51300	0.09015	-0.05234
0.53573	0.08770	-0.05134
0.55845	0.08522	-0.05019
0.58118	0.08194	-0.04766
0.60391	0.07822	-0.04470
0.62664	0.07404	-0.04132
0.64936	0.06945	-0.03767
0.67209	0.06451	-0.03383
0.69482	0.05925	-0.02988
0.71755	0.05375	-0.02588
0.74027	0.04745	-0.02174
0.76300	0.04222	-0.01793
0.78573	0.03621	-0.01402
0.80845	0.03012	-0.01052
0.83118	0.02399	-0.00752
0.85391	0.01875	-0.00550
0.87664	0.01363	-0.00466
0.89936	0.00951	-0.00466
0.91559	0.00700	-0.00475
0.93182	0.00500	-0.00420
0.94319	0.00425	-0.00400
0.95455	0.00375	-0.00380
0.96591	0.00330	-0.00300
0.97727	0.00415	-0.00100
0.98864	0.00550	0.00100
1.00000	0.00700	0.00700
1.00000	0.00500	0.00500
1.00000	0.00300	0.00300

APPENDIX C

COORDINATES FOR SD 8020 AIRFOIL SECTION

Coordinates for SD 8020 Airfoil Section

X	Y_{upper}	X	Y_{lower}
0.0000	0.0000	0.0000	0.00000
.00276	.00645	.00276	-.00645
.01065	.01345	.01066	-.01345
.02318	.02041	.02319	-.02041
.04024	.02697	.04024	-.02697
.06179	.03287	.06180	-.03287
.08774	.03802	.08774	-.03802
.11789	.04233	.11790	-.04233
.15203	.04574	.15204	-.04574
.18987	.04824	.18987	-.04824
.23106	.04982	.23107	-.04982
.27523	.05051	.27524	-.05051
.32196	.05034	.32197	-.05034
.37077	.04938	.37077	-.04938
.42116	.04770	.42117	-.04769
.47261	.04536	.47262	-.04536
.52456	.04246	.52457	-.04246
.57647	.03909	.57648	-.03908
.62777	.03535	.62778	-.03534
.67789	.03135	.67790	-.03135
.72627	.02722	.72629	-.02722
.77237	.02308	.77238	-.02308
.81560	.01908	.81561	-.01907
.85538	.01532	.85539	-.01532
.89118	.01188	.89119	-.01188
.92247	.00876	.92248	-.00876
.94885	.00591	.94886	-.00591
.97017	.00330	.97018	-.00330
.98625	.00131	.98626	-.00131
.99646	.00027	.99647	-.00027
1.00000	0.00000	1.00000	0.00000

APPENDIX D

AERODYNAMIC DATA FOR AIRCRAFT

Gamma air	density (lbm/ft^3)	Temp Cruis (F)	R (ft*lbf/lbm*R)	Speed of Sound (ft/s)
1.4	0.0764743	59.02	53.34	1116.792264
1.4	0.0764743	59.02	53.34	1116.792264
1.4	0.0764743	59.02	53.34	1116.792264
1.4	0.0764743	59.02	53.34	1116.792264
1.4	0.0764743	59.02	53.34	1116.792264
1.4	0.0764743	59.02	53.34	1116.792264
1.4	0.0764743	59.02	53.34	1116.792264
1.4	0.0764743	59.02	53.34	1116.792264
1.4	0.0764743	59.02	53.34	1116.792264
1.4	0.0764743	59.02	53.34	1116.792264
1.4	0.0764743	59.02	53.34	1116.792264
1.4	0.0764743	59.02	53.34	1116.792264
1.4	0.0764743	59.02	53.34	1116.792264
1.4	0.0764743	59.02	53.34	1116.792264
1.4	0.0764743	59.02	53.34	1116.792264
1.4	0.0764743	59.02	53.34	1116.792264
1.4	0.0764743	59.02	53.34	1116.792264
1.4	0.0764743	59.02	53.34	1116.792264
1.4	0.0764743	59.02	53.34	1116.792264
1.4	0.0764743	59.02	53.34	1116.792264
1.4	0.0764743	59.02	53.34	1116.792264
1.4	0.0764743	59.02	53.34	1116.792264
1.4	0.0764743	59.02	53.34	1116.792264
1.4	0.0764743	59.02	53.34	1116.792264
1.4	0.0764743	59.02	53.34	1116.792264
1.4	0.0764743	59.02	53.34	1116.792264
1.4	0.0764743	59.02	53.34	1116.792264
1.4	0.0764743	59.02	53.34	1116.792264
1.4	0.0764743	59.02	53.34	1116.792264
1.4	0.0764743	59.02	53.34	1116.792264
1.4	0.0764743	59.02	53.34	1116.792264
1.4	0.0764743	59.02	53.34	1116.792264
1.4	0.0764743	59.02	53.34	1116.792264
1.4	0.0764743	59.02	53.34	1116.792264
1.4	0.0764743	59.02	53.34	1116.792264
1.4	0.0764743	59.02	53.34	1116.792264
1.4	0.0764743	59.02	53.34	1116.792264
1.4	0.0764743	59.02	53.34	1116.792264
1.4	0.0764743	59.02	53.34	1116.792264
1.4	0.0764743	59.02	53.34	1116.792264
1.4	0.0764743	59.02	53.34	1116.792264
1.4	0.0764743	59.02	53.34	1116.792264
1.4	0.0764743	59.02	53.34	1116.792264
1.4	0.0764743	59.02	53.34	1116.792264
1.4	0.0764743	59.02	53.34	1116.792264
1.4	0.0764743	59.02	53.34	1116.792264
1.4	0.0764743	59.02	53.34	1116.792264
1.4	0.0764743	59.02	53.34	1116.792264
1.4	0.0764743	59.02	53.34	1116.792264
1.4	0.0764743	59.02	53.34	1116.792264

V Cruise (m/s)	V Cruise (ft/s)	Mach Cruise	Beta	Cl alpha section
0	0	0	1	6.97
4	13.12335958	0.011750940621	0.99986191539	6.97
8	26.24671916	0.023501881241	0.99944766158	6.97
12	39.37007874	0.035252821862	0.99875723855	6.97
16	52.49343832	0.047003762483	0.99779064631	6.97
20	65.6167979	0.058754703103	0.99654788486	6.97
0	0	0	1	6.97
4	13.12335958	0.011750940621	0.99986191539	6.97
8	26.24671916	0.023501881241	0.99944766158	6.97
12	39.37007874	0.035252821862	0.99875723855	6.97
16	52.49343832	0.047003762483	0.99779064631	6.97
20	65.6167979	0.058754703103	0.99654788486	6.97
0	0	0	1	6.97
1	3.280839895	0.002937735155	0.99999136971	6.97
2	6.56167979	0.00587547031	0.99996547885	6.97
3	9.842519685	0.008813205465	0.99992232741	6.97
4	13.12335958	0.011750940621	0.99986191539	6.97
5	16.404199475	0.014688675776	0.9997842428	6.97
6	19.68503937	0.017626410931	0.99968930964	6.97
7	22.965879265	0.020564146086	0.9995771159	6.97
8	26.24671916	0.023501881241	0.99944766158	6.97
9	29.527559055	0.026439616396	0.99930094668	6.97
10	32.80839895	0.029377351552	0.99913697122	6.97
11	36.089238845	0.032315086707	0.99895573517	6.97
12	39.37007874	0.035252821862	0.99875723855	6.97
13	42.650918635	0.038190557017	0.99854148135	6.97
14	45.93175853	0.041128292172	0.99830846358	6.97
15	49.212598425	0.044066027327	0.99805818524	6.97
16	52.49343832	0.047003762483	0.99779064631	6.97
17	55.774278215	0.049941497638	0.99750584681	6.97
18	59.05511811	0.052879232793	0.99720378674	6.97
19	62.335958005	0.055816967948	0.99688446609	6.97
20	65.6167979	0.058754703103	0.99654788486	6.97
0	0	0	1	6.97
4	13.12335958	0.011750940621	0.99986191539	6.97
8	26.24671916	0.023501881241	0.99944766158	6.97
12	39.37007874	0.035252821862	0.99875723855	6.97
16	52.49343832	0.047003762483	0.99779064631	6.97
20	65.6167979	0.058754703103	0.99654788486	6.97
0	0	0	1	6.97
4	13.12335958	0.011750940621	0.99986191539	6.97
8	26.24671916	0.023501881241	0.99944766158	6.97
12	39.37007874	0.035252821862	0.99875723855	6.97
16	52.49343832	0.047003762483	0.99779064631	6.97
20	65.6167979	0.058754703103	0.99654788486	6.97
4	13.12335958	0.011750940621	0.99986191539	6.97
8	26.24671916	0.023501881241	0.99944766158	6.97
12	39.37007874	0.035252821862	0.99875723855	6.97
16	52.49343832	0.047003762483	0.99779064631	6.97
20	65.6167979	0.058754703103	0.99654788486	6.97

Sref (ft^2)	C root (ft)	Sexposed (ft^2)	Aspect eff	Sweep t/c max	CL alpha	Alpha not (deg)
9.6106343	1.46	9.6106343	7	0	5.0711746426	1
9.6106343	1.46	9.6106343	7	0	5.0716825682	1
9.6106343	1.46	9.6106343	7	0	5.0732069238	1
9.6106343	1.46	9.6106343	7	0	5.0757494475	1
9.6106343	1.46	9.6106343	7	0	5.0793130414	1
9.6106343	1.46	9.6106343	7	0	5.0839017787	1
9.6106343	1.46	9.6106343	7	0	5.0711746426	1
9.6106343	1.46	9.6106343	7	0	5.0716825682	1
9.6106343	1.46	9.6106343	7	0	5.0732069238	1
9.6106343	1.46	9.6106343	7	0	5.0757494475	1
9.6106343	1.46	9.6106343	7	0	5.0793130414	1
9.6106343	1.46	9.6106343	7	0	5.0839017787	1
9.6106343	1.46	9.6106343	7	0	5.0711746426	1
9.6106343	1.46	9.6106343	7	0	5.0712063851	1
9.6106343	1.46	9.6106343	7	0	5.0713016149	1
9.6106343	1.46	9.6106343	7	0	5.0714603388	1
9.6106343	1.46	9.6106343	7	0	5.0716825682	1
9.6106343	1.46	9.6106343	7	0	5.0719683187	1
9.6106343	1.46	9.6106343	7	0	5.0723176108	1
9.6106343	1.46	9.6106343	7	0	5.0727304693	1
9.6106343	1.46	9.6106343	7	0	5.0732069238	1
9.6106343	1.46	9.6106343	7	0	5.073747008	1
9.6106343	1.46	9.6106343	7	0	5.0743507606	1
9.6106343	1.46	9.6106343	7	0	5.0750182246	1
9.6106343	1.46	9.6106343	7	0	5.0757494475	1
9.6106343	1.46	9.6106343	7	0	5.0765444817	1
9.6106343	1.46	9.6106343	7	0	5.0774033837	1
9.6106343	1.46	9.6106343	7	0	5.078326215	1
9.6106343	1.46	9.6106343	7	0	5.0793130414	1
9.6106343	1.46	9.6106343	7	0	5.0803639335	1
9.6106343	1.46	9.6106343	7	0	5.0814789665	1
9.6106343	1.46	9.6106343	7	0	5.0826582201	1
9.6106343	1.46	9.6106343	7	0	5.0839017787	1
9.6106343	1.46	9.6106343	7	0	5.0711746426	1
9.6106343	1.46	9.6106343	7	0	5.0716825682	1
9.6106343	1.46	9.6106343	7	0	5.0732069238	1
9.6106343	1.46	9.6106343	7	0	5.0757494475	1
9.6106343	1.46	9.6106343	7	0	5.0793130414	1
9.6106343	1.46	9.6106343	7	0	5.0839017787	1
9.6106343	1.46	9.6106343	7	0	5.0711746426	1
9.6106343	1.46	9.6106343	7	0	5.0716825682	1
9.6106343	1.46	9.6106343	7	0	5.0732069238	1
9.6106343	1.46	9.6106343	7	0	5.0757494475	1
9.6106343	1.46	9.6106343	7	0	5.0793130414	1
9.6106343	1.46	9.6106343	7	0	5.0839017787	1
9.6106343	1.46	9.6106343	7	0	5.0716825682	1
9.6106343	1.46	9.6106343	7	0	5.0732069238	1
9.6106343	1.46	9.6106343	7	0	5.0757494475	1
9.6106343	1.46	9.6106343	7	0	5.0793130414	1
9.6106343	1.46	9.6106343	7	0	5.0839017787	1

Cl not	Cruise angle	Alpha crui (rad)	**CL** (wing)	q*S (lbf)	L wing	L (N)
0.081	0	0	0.081	0	0	0
0.081	0	0	0.081	1.9654941	0.159205	0.7081792
0.081	0	0	0.081	7.8619765	0.6368201	2.8327169
0.081	0	0	0.081	17.689447	1.4328452	6.3736131
0.081	0	0	0.081	31.447906	2.5472804	11.330868
0.081	0	0	0.081	49.137353	3.9801256	17.704481
0.081	2	0.0349066	0.25801738891	0	0	0
0.081	2	0.0349066	0.25803511886	1.9654941	0.5071665	2.255989
0.081	2	0.0349066	0.25808832891	7.8619765	2.0290844	9.025817
0.081	2	0.0349066	0.25817707973	17.689447	4.5670098	20.315072
0.081	2	0.0349066	0.25830147262	31.447906	8.1230405	36.133084
0.081	2	0.0349066	0.25846164977	49.137353	12.700121	56.492955
0.081	4	0.0698132	0.43503477783	0	0	0
0.081	4	0.0698132	0.43503699387	0.1228434	0.0534414	0.2377193
0.081	4	0.0698132	0.43504364217	0.4913735	0.2137689	0.9508916
0.081	4	0.0698132	0.43505472319	1.1055905	0.4809923	2.1395606
0.081	4	0.0698132	0.43507023772	1.9654941	0.855128	3.8037989
0.081	4	0.0698132	0.43509018687	3.0710846	1.3361988	5.9437082
0.081	4	0.0698132	0.43511457206	4.4223618	1.9242341	8.5594196
0.081	4	0.0698132	0.43514339503	6.0193258	2.6192699	11.651093
0.081	4	0.0698132	0.43517665782	7.8619765	3.4213487	15.218917
0.081	4	0.0698132	0.43521436281	9.9503141	4.3305196	19.263111
0.081	4	0.0698132	0.4352565127	12.284338	5.3468383	23.783922
0.081	4	0.0698132	0.43530311047	14.864049	6.4703669	28.781626
0.081	4	0.0698132	0.43535415946	17.689447	7.7011744	34.256531
0.081	4	0.0698132	0.43540966332	20.760532	9.0393362	40.208971
0.081	4	0.0698132	0.43546962599	24.077303	10.484934	46.639311
0.081	4	0.0698132	0.43553405176	27.639761	12.038057	53.547946
0.081	4	0.0698132	0.43560294525	31.447906	13.698801	60.935301
0.081	4	0.0698132	0.43567631136	35.501738	15.467266	68.801828
0.081	4	0.0698132	0.43575415534	39.801256	17.343563	77.148011
0.081	4	0.0698132	0.43583648278	44.346461	19.327806	85.974363
0.081	4	0.0698132	0.43592329955	49.137353	21.420117	95.281428
0.081	6	0.1047198	0.61205216674	0	0	0
0.081	6	0.1047198	0.61210535658	1.9654941	1.2030895	5.3516087
0.081	6	0.1047198	0.61226498673	7.8619765	4.813613	21.412017
0.081	6	0.1047198	0.6125312392	17.689447	10.835339	48.197989
0.081	6	0.1047198	0.61290441787	31.447906	19.274561	85.737517
0.081	6	0.1047198	0.61338494932	49.137353	30.140113	134.0699
0.081	6	0.1047198	0.61205216674	0	0	0
0.081	8	0.1396263	0.78914047544	1.9654941	1.551051	6.8994185
0.081	8	0.1396263	0.78935331564	7.8619765	6.2058773	27.605117
0.081	8	0.1396263	0.78970831893	17.689447	13.969504	62.139448
0.081	8	0.1396263	0.79020589049	31.447906	24.850321	110.53973
0.081	8	0.1396263	0.79084659909	49.137353	38.860109	172.85838
0.081	10	0.1745329	0.9661755943	1.9654941	1.8990125	8.4472283
0.081	10	0.1745329	0.96644164455	7.8619765	7.5981415	33.798217
0.081	10	0.1745329	0.96688539866	17.689447	17.103668	76.080907
0.081	10	0.1745329	0.96750736312	31.447906	30.426081	135.34195
0.081	10	0.1745329	0.96830824887	49.137353	47.580105	211.64685

Weight guess (N)	Kinematic viscosity	Cf skin friction	l wing (ft)	l VT (ft)	Re wing	Re VT
55	0.0001572		1.46	0.43175	0	0
55	0.0001572		1.46	0.43175	121862.1	36036.961
55	0.0001572		1.46	0.43175	243724.21	72073.922
55	0.0001572		1.46	0.43175	365586.31	108110.88
55	0.0001572		1.46	0.43175	487448.41	144147.84
55	0.0001572		1.46	0.43175	609310.52	180184.81
55	0.0001572		1.46	0.43175	0	0
55	0.0001572		1.46	0.43175	121862.1	36036.961
55	0.0001572		1.46	0.43175	243724.21	72073.922
55	0.0001572		1.46	0.43175	365586.31	108110.88
55	0.0001572		1.46	0.43175	487448.41	144147.84
55	0.0001572		1.46	0.43175	609310.52	180184.81
55	0.0001572		1.46	0.43175	0	0
55	0.0001572		1.46	0.43175	30465.526	9009.2403
55	0.0001572		1.46	0.43175	60931.052	18018.481
55	0.0001572		1.46	0.43175	91396.578	27027.721
55	0.0001572		1.46	0.43175	121862.1	36036.961
55	0.0001572		1.46	0.43175	152327.63	45046.201
55	0.0001572		1.46	0.43175	182793.16	54055.442
55	0.0001572		1.46	0.43175	213258.68	63064.682
55	0.0001572		1.46	0.43175	243724.21	72073.922
55	0.0001572		1.46	0.43175	274189.73	81083.163
55	0.0001572		1.46	0.43175	304655.26	90092.403
55	0.0001572		1.46	0.43175	335120.79	99101.643
55	0.0001572		1.46	0.43175	365586.31	108110.88
55	0.0001572		1.46	0.43175	396051.84	117120.12
55	0.0001572		1.46	0.43175	426517.36	126129.36
55	0.0001572		1.46	0.43175	456982.89	135138.6
55	0.0001572		1.46	0.43175	487448.41	144147.84
55	0.0001572		1.46	0.43175	517913.94	153157.08
55	0.0001572		1.46	0.43175	548379.47	162166.33
55	0.0001572		1.46	0.43175	578844.99	171175.57
55	0.0001572		1.46	0.43175	609310.52	180184.81
55	0.0001572		1.46	0.43175	0	0
55	0.0001572		1.46	0.43175	121862.1	36036.961
55	0.0001572		1.46	0.43175	243724.21	72073.922
55	0.0001572		1.46	0.43175	365586.31	108110.88
55	0.0001572		1.46	0.43175	487448.41	144147.84
55	0.0001572		1.46	0.43175	609310.52	180184.81
55	0.0001572		1.46	0.43175	0	0
55	0.0001572		1.46	0.43175	121862.1	36036.961
55	0.0001572		1.46	0.43175	243724.21	72073.922
55	0.0001572		1.46	0.43175	365586.31	108110.88
55	0.0001572		1.46	0.43175	487448.41	144147.84
55	0.0001572		1.46	0.43175	609310.52	180184.81
55	0.0001572		1.46	0.43175	121862.1	36036.961
55	0.0001572		1.46	0.43175	243724.21	72073.922
55	0.0001572		1.46	0.43175	365586.31	108110.88
55	0.0001572		1.46	0.43175	487448.41	144147.84
55	0.0001572		1.46	0.43175	609310.52	180184.81

Re nacelle	Cf wing	Cf VT	Cf nacelle	FF factors	t/c wing	t/c VT
0	ERR	ERR	ERR		0.15	0.1011
121862.1	0.0068483	0.0090923	0.0068483		0.15	0.1011
243724.21	0.0059038	0.0077087	0.0059038		0.15	0.1011
365586.31	0.0054333	0.0070316	0.0054333		0.15	0.1011
487448.41	0.0051303	0.0066	0.0051303		0.15	0.1011
609310.52	0.0049109	0.0062899	0.0049109		0.15	0.1011
0	ERR	ERR	ERR		0.15	0.1011
121862.1	0.0068483	0.0090923	0.0068483		0.15	0.1011
243724.21	0.0059038	0.0077087	0.0059038		0.15	0.1011
365586.31	0.0054333	0.0070316	0.0054333		0.15	0.1011
487448.41	0.0051303	0.0066	0.0051303		0.15	0.1011
609310.52	0.0049109	0.0062899	0.0049109		0.15	0.1011
0	ERR	ERR	ERR		0.15	0.1011
30465.526	0.009479	0.0131057	0.009479		0.15	0.1011
60931.052	0.0080159	0.0108458	0.0080159		0.15	0.1011
91396.578	0.0073022	0.0097685	0.0073022		0.15	0.1011
121862.1	0.0068483	0.0090923	0.0068483		0.15	0.1011
152327.63	0.0065228	0.0086118	0.0065228		0.15	0.1011
182793.16	0.0062725	0.0082449	0.0062725		0.15	0.1011
213258.68	0.0060711	0.0079514	0.0060711		0.15	0.1011
243724.21	0.0059038	0.0077087	0.0059038		0.15	0.1011
274189.73	0.0057615	0.007503	0.0057615		0.15	0.1011
304655.26	0.0056382	0.0073254	0.0056382		0.15	0.1011
335120.79	0.0055298	0.0071698	0.0055298		0.15	0.1011
365586.31	0.0054333	0.0070316	0.0054333		0.15	0.1011
396051.84	0.0053466	0.0069077	0.0053466		0.15	0.1011
426517.36	0.005268	0.0067957	0.005268		0.15	0.1011
456982.89	0.0051962	0.0066936	0.0051962		0.15	0.1011
487448.41	0.0051303	0.0066	0.0051303		0.15	0.1011
517913.94	0.0050694	0.0065137	0.0050694		0.15	0.1011
548379.47	0.0050128	0.0064338	0.0050128		0.15	0.1011
578844.99	0.0049602	0.0063594	0.0049602		0.15	0.1011
609310.52	0.0049109	0.0062899	0.0049109		0.15	0.1011
0	ERR	ERR	ERR		0.15	0.1011
121862.1	0.0068483	0.0090923	0.0068483		0.15	0.1011
243724.21	0.0059038	0.0077087	0.0059038		0.15	0.1011
365586.31	0.0054333	0.0070316	0.0054333		0.15	0.1011
487448.41	0.0051303	0.0066	0.0051303		0.15	0.1011
609310.52	0.0049109	0.0062899	0.0049109		0.15	0.1011
0	ERR	ERR	ERR		0.15	0.1011
121862.1	0.0068483	0.0090923	0.0068483		0.15	0.1011
243724.21	0.0059038	0.0077087	0.0059038		0.15	0.1011
365586.31	0.0054333	0.0070316	0.0054333		0.15	0.1011
487448.41	0.0051303	0.0066	0.0051303		0.15	0.1011
609310.52	0.0049109	0.0062899	0.0049109		0.15	0.1011
121862.1	0.0068483	0.0090923	0.0068483		0.15	0.1011
243724.21	0.0059038	0.0077087	0.0059038		0.15	0.1011
365586.31	0.0054333	0.0070316	0.0054333		0.15	0.1011
487448.41	0.0051303	0.0066	0.0051303		0.15	0.1011
609310.52	0.0049109	0.0062899	0.0049109		0.15	0.1011

d nacelle (ft)	f nacelle	FF nacelle	Q wing	Q VT	Q nacelle	Sw wing (ft^2)
0.42	3.4761905	1.1006849	1	1	1.3	19.413481
0.42	3.4761905	1.1006849	1	1	1.3	19.413481
0.42	3.4761905	1.1006849	1	1	1.3	19.413481
0.42	3.4761905	1.1006849	1	1	1.3	19.413481
0.42	3.4761905	1.1006849	1	1	1.3	19.413481
0.42	3.4761905	1.1006849	1	1	1.3	19.413481
0.42	3.4761905	1.1006849	1	1	1.3	19.413481
0.42	3.4761905	1.1006849	1	1	1.3	19.413481
0.42	3.4761905	1.1006849	1	1	1.3	19.413481
0.42	3.4761905	1.1006849	1	1	1.3	19.413481
0.42	3.4761905	1.1006849	1	1	1.3	19.413481
0.42	3.4761905	1.1006849	1	1	1.3	19.413481
0.42	3.4761905	1.1006849	1	1	1.3	19.413481
0.42	3.4761905	1.1006849	1	1	1.3	19.413481
0.42	3.4761905	1.1006849	1	1	1.3	19.413481
0.42	3.4761905	1.1006849	1	1	1.3	19.413481
0.42	3.4761905	1.1006849	1	1	1.3	19.413481
0.42	3.4761905	1.1006849	1	1	1.3	19.413481
0.42	3.4761905	1.1006849	1	1	1.3	19.413481
0.42	3.4761905	1.1006849	1	1	1.3	19.413481
0.42	3.4761905	1.1006849	1	1	1.3	19.413481
0.42	3.4761905	1.1006849	1	1	1.3	19.413481
0.42	3.4761905	1.1006849	1	1	1.3	19.413481
0.42	3.4761905	1.1006849	1	1	1.3	19.413481
0.42	3.4761905	1.1006849	1	1	1.3	19.413481
0.42	3.4761905	1.1006849	1	1	1.3	19.413481
0.42	3.4761905	1.1006849	1	1	1.3	19.413481
0.42	3.4761905	1.1006849	1	1	1.3	19.413481
0.42	3.4761905	1.1006849	1	1	1.3	19.413481
0.42	3.4761905	1.1006849	1	1	1.3	19.413481
0.42	3.4761905	1.1006849	1	1	1.3	19.413481
0.42	3.4761905	1.1006849	1	1	1.3	19.413481
0.42	3.4761905	1.1006849	1	1	1.3	19.413481
0.42	3.4761905	1.1006849	1	1	1.3	19.413481
0.42	3.4761905	1.1006849	1	1	1.3	19.413481
0.42	3.4761905	1.1006849	1	1	1.3	19.413481
0.42	3.4761905	1.1006849	1	1	1.3	19.413481
0.42	3.4761905	1.1006849	1	1	1.3	19.413481
0.42	3.4761905	1.1006849	1	1	1.3	19.413481
0.42	3.4761905	1.1006849	1	1	1.3	19.413481
0.42	3.4761905	1.1006849	1	1	1.3	19.413481
0.42	3.4761905	1.1006849	1	1	1.3	19.413481
0.42	3.4761905	1.1006849	1	1	1.3	19.413481
0.42	3.4761905	1.1006849	1	1	1.3	19.413481
0.42	3.4761905	1.1006849	1	1	1.3	19.413481
0.42	3.4761905	1.1006849	1	1	1.3	19.413481
0.42	3.4761905	1.1006849	1	1	1.3	19.413481
0.42	3.4761905	1.1006849	1	1	1.3	19.413481
0.42	3.4761905	1.1006849	1	1	1.3	19.413481
0.42	3.4761905	1.1006849	1	1	1.3	19.413481

Sw VT (ft^2)	Sw nacelle (ft^2)	Cp wing	Cp VT	Cp nacelle	Cp Total/S	Leak & Protrub
1.17	0.9632123	ERR	ERR	ERR	ERR	ERR
1.17	0.9632123	0.1021241	0.0151776	0.0188774	0.0141696	0.0002834
1.17	0.9632123	0.0997389	0.0145778	0.016274	0.0135881	0.0002718
1.17	0.9632123	0.0987397	0.0143042	0.014977	0.0133207	0.0002664
1.17	0.9632123	0.0981872	0.0141398	0.0141416	0.0131592	0.0002632
1.17	0.9632123	0.0978405	0.0140276	0.0135369	0.0130486	0.000261
1.17	0.9632123	ERR	ERR	ERR	ERR	ERR
1.17	0.9632123	0.1021241	0.0151776	0.0188774	0.0141696	0.0002834
1.17	0.9632123	0.0997389	0.0145778	0.016274	0.0135881	0.0002718
1.17	0.9632123	0.0987397	0.0143042	0.014977	0.0133207	0.0002664
1.17	0.9632123	0.0981872	0.0141398	0.0141416	0.0131592	0.0002632
1.17	0.9632123	0.0978405	0.0140276	0.0135369	0.0130486	0.000261
1.17	0.9632123	ERR	ERR	ERR	ERR	ERR
1.17	0.9632123	0.1101375	0.0170458	0.0261288	0.0159523	0.000319
1.17	0.9632123	0.1055143	0.0159809	0.0220959	0.0149409	0.0002988
1.17	0.9632123	0.1033977	0.0154834	0.0201286	0.0144642	0.0002893
1.17	0.9632123	0.1021241	0.0151776	0.0188774	0.0141696	0.0002834
1.17	0.9632123	0.1012556	0.0149646	0.01798	0.0139637	0.0002793
1.17	0.9632123	0.1006187	0.014805	0.0172901	0.0138091	0.0002762
1.17	0.9632123	0.1001288	0.0146796	0.016735	0.0136873	0.0002737
1.17	0.9632123	0.0997389	0.0145778	0.016274	0.0135881	0.0002718
1.17	0.9632123	0.0994206	0.0144929	0.0158817	0.0135054	0.0002701
1.17	0.9632123	0.0991557	0.0144208	0.0155418	0.0134349	0.0002687
1.17	0.9632123	0.0989316	0.0143586	0.015243	0.0133741	0.0002675
1.17	0.9632123	0.0987397	0.0143042	0.014977	0.0133207	0.0002664
1.17	0.9632123	0.0985735	0.0142561	0.0147379	0.0132736	0.0002655
1.17	0.9632123	0.0984283	0.0142132	0.0145212	0.0132315	0.0002646
1.17	0.9632123	0.0983005	0.0141746	0.0143233	0.0131936	0.0002639
1.17	0.9632123	0.0981872	0.0141398	0.0141416	0.0131592	0.0002632
1.17	0.9632123	0.0980862	0.014108	0.0139737	0.013128	0.0002626
1.17	0.9632123	0.0979957	0.0140789	0.0138179	0.0130993	0.000262
1.17	0.9632123	0.0979142	0.0140522	0.0136727	0.0130729	0.0002615
1.17	0.9632123	0.0978405	0.0140276	0.0135369	0.0130486	0.000261
1.17	0.9632123	ERR	ERR	ERR	ERR	ERR
1.17	0.9632123	0.1021241	0.0151776	0.0188774	0.0141696	0.0002834
1.17	0.9632123	0.0997389	0.0145778	0.016274	0.0135881	0.0002718
1.17	0.9632123	0.0987397	0.0143042	0.014977	0.0133207	0.0002664
1.17	0.9632123	0.0981872	0.0141398	0.0141416	0.0131592	0.0002632
1.17	0.9632123	0.0978405	0.0140276	0.0135369	0.0130486	0.000261
1.17	0.9632123	ERR	ERR	ERR	ERR	ERR
1.17	0.9632123	0.1021241	0.0151776	0.0188774	0.0141696	0.0002834
1.17	0.9632123	0.0997389	0.0145778	0.016274	0.0135881	0.0002718
1.17	0.9632123	0.0987397	0.0143042	0.014977	0.0133207	0.0002664
1.17	0.9632123	0.0981872	0.0141398	0.0141416	0.0131592	0.0002632
1.17	0.9632123	0.0978405	0.0140276	0.0135369	0.0130486	0.000261
1.17	0.9632123	0.1021241	0.0151776	0.0188774	0.0141696	0.0002834
1.17	0.9632123	0.0997389	0.0145778	0.016274	0.0135881	0.0002718
1.17	0.9632123	0.0987397	0.0143042	0.014977	0.0133207	0.0002664
1.17	0.9632123	0.0981872	0.0141398	0.0141416	0.0131592	0.0002632
1.17	0.9632123	0.0978405	0.0140276	0.0135369	0.0130486	0.000261

CDo ****	e	K -	CDi cruise	**CD** cruise
ERR	1	0.0454728	0.0002983	ERR
0.014453	1	0.0454728	0.0002983	0.0147514
0.0138599	1	0.0454728	0.0002983	0.0141583
0.0135872	1	0.0454728	0.0002983	0.0138855
0.0134224	1	0.0454728	0.0002983	0.0137208
0.0133095	1	0.0454728	0.0002983	0.0136079
ERR	1	0.0454728	0.0030273	ERR
0.014453	1	0.0454728	0.0030277	0.0174807
0.0138599	1	0.0454728	0.0030289	0.0168888
0.0135872	1	0.0454728	0.003031	0.0166182
0.0134224	1	0.0454728	0.0030339	0.0164564
0.0133095	1	0.0454728	0.0030377	0.0163472
ERR	1	0.0454728	0.008606	ERR
0.0162714	1	0.0454728	0.0086061	0.0248774
0.0152397	1	0.0454728	0.0086063	0.023846
0.0147534	1	0.0454728	0.0086068	0.0233602
0.014453	1	0.0454728	0.0086074	0.0230604
0.014243	1	0.0454728	0.0086082	0.0228512
0.0140852	1	0.0454728	0.0086091	0.0226944
0.013961	1	0.0454728	0.0086103	0.0225713
0.0138599	1	0.0454728	0.0086116	0.0224715
0.0137755	1	0.0454728	0.0086131	0.0223886
0.0137036	1	0.0454728	0.0086147	0.0223184
0.0136415	1	0.0454728	0.0086166	0.0222581
0.0135872	1	0.0454728	0.0086186	0.0222058
0.013539	1	0.0454728	0.0086208	0.0221599
0.0134961	1	0.0454728	0.0086232	0.0221193
0.0134574	1	0.0454728	0.0086257	0.0220832
0.0134224	1	0.0454728	0.0086285	0.0220509
0.0133905	1	0.0454728	0.0086314	0.0220219
0.0133613	1	0.0454728	0.0086345	0.0219957
0.0133344	1	0.0454728	0.0086377	0.0219721
0.0133095	1	0.0454728	0.0086412	0.0219507
ERR	1	0.0454728	0.0170345	ERR
0.014453	1	0.0454728	0.0170374	0.0314905
0.0138599	1	0.0454728	0.0170463	0.0309062
0.0135872	1	0.0454728	0.0170612	0.0306483
0.0134224	1	0.0454728	0.017082	0.0305044
0.0133095	1	0.0454728	0.0171088	0.0304183
ERR	1	0.0454728	0.0170345	ERR
0.014453	1	0.0454728	0.0283179	0.0427709
0.0138599	1	0.0454728	0.0283332	0.0421931
0.0135872	1	0.0454728	0.0283586	0.0419458
0.0134224	1	0.0454728	0.0283944	0.0418168
0.0133095	1	0.0454728	0.0284405	0.04175
0.014453	1	0.0454728	0.0424487	0.0569017
0.0138599	1	0.0454728	0.0424721	0.056332
0.0135872	1	0.0454728	0.0425111	0.0560982
0.0134224	1	0.0454728	0.0425658	0.0559882
0.0133095	1	0.0454728	0.0426363	0.0559458

Drag cru (lbf)	Drag (N)	--L/D-- cruise
ERR	ERR	ERR
0.0023485	0.0104466	5.4910191
0.0090163	0.0401061	5.7210455
0.0198958	0.0885004	5.8334202
0.0349506	0.1554674	5.9034604
0.0541611	0.2409192	5.9524358
ERR	ERR	ERR
0.0088656	0.0394361	14.761151
0.0342689	0.1524348	15.281598
0.0758953	0.3375977	15.53583
0.1336756	0.5946158	15.696157
0.2076117	0.9234985	15.810737
ERR	ERR	ERR
0.0013295	0.0059138	17.487202
0.0050975	0.0226748	18.243889
0.0112361	0.0499803	18.623756
0.0197196	0.0877167	18.86656
0.0305337	0.1358199	19.040184
0.0436693	0.1942497	19.172799
0.0591203	0.262979	19.278614
0.0768828	0.3419901	19.365721
0.0969541	0.4312714	19.439131
0.1193328	0.5308163	19.502145
0.1440183	0.640622	19.557039
0.1710105	0.7606891	19.605447
0.2003104	0.8910208	19.648576
0.2319191	1.0316227	19.687337
0.2658385	1.1825028	19.72244
0.3020707	1.3436709	19.754441
0.3406184	1.5151387	19.783787
0.3814846	1.6969197	19.810839
0.4246727	1.8890289	19.835897
0.4701864	2.0914831	19.859206
ERR	ERR	ERR
0.0378858	0.1685238	19.437805
0.1487707	0.6617616	19.810403
0.3320849	1.4771803	19.985801
0.5879584	2.6153566	20.092345
0.9168104	4.0781559	20.165012
ERR	ERR	ERR
0.0663398	0.2950928	18.45041
0.261845	1.1647387	18.708131
0.5859621	2.6064767	18.826871
1.0391612	4.6223969	18.896846
1.622409	7.2167996	18.94244
0.108057	0.4806593	16.979733
0.4280183	1.9039108	17.156185
0.9594856	4.2679839	17.235576
1.7035016	7.5775158	17.280557
2.6619076	11.840697	17.307967

APPENDIX E

MATHCAD RESULTS FOR

STRUCTURAL ANAYLSIS

Read Pints from data file (hp33.prn-section points, hp33int.prn-lift, drag, moment)

$i := 0..45 \qquad j := 0..12$

$point := READPRN(points) \qquad LDM := READPRN(ldm)$

$x_{u_i} := point_{i+45,0} \qquad y_{u_i} := point_{i+45,1} \qquad y_{l_i} := point_{45-i,1} \qquad x_{u_{44,0}} := 0.999$

$x_l := x_u$

$Lift := 65.769$ **Span:** $s := 1.25 \qquad z1 := 0, 0.25..1.25 \qquad N \equiv newton$

$$y(z) := \frac{Lift}{2}\cdot\left[1-\left(\frac{s-z}{s}\right)^2\right]^{0.5}$$ Equation for the elliptical distribution of lift across the span of the wing

$$y(z) := \frac{Lift}{2}\cdot\sqrt{z}\cdot\frac{\sqrt{2.\cdot s - 1.\cdot z}}{s} \qquad v(z) := \int_0^z y(z)\,dz \qquad M(z) := \int_0^z v(z)\,dz$$

Force

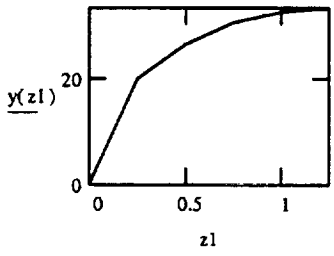

Shear

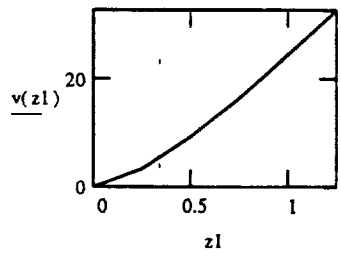

Moment

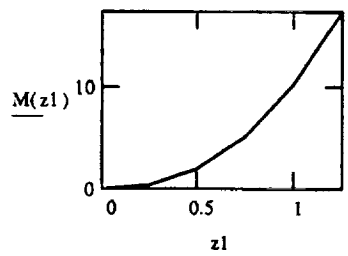

Polynomial fit of: Force, Shear and Moment curves

$Rows := 9 \quad k := 0..Rows \quad z_{f_k} := k\cdot 0.125 \quad y_{f_k} := y\left(z_{f_k}\right) \quad degree := 5 \quad i := 0..degree \quad point := 0..Rows$

$$z\,matrix_{(point,i)} := \left[z_{f_{(point,0)}}\right]^i \qquad y_{f\_coeff} := \left(z\,matrix^T\cdot z\,matrix\right)^{-1}\cdot z\,matrix^T\cdot y_f$$

$$y_{f\_eq}(z) := \left(\sum_i y_{f\_coeff_i}\cdot z^i\right)\cdot N$$

Force

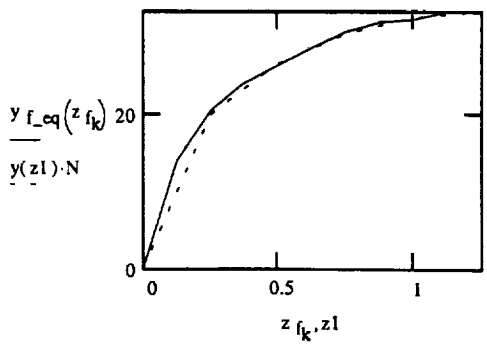

$$y_{f\_coeff} = \begin{bmatrix} 0.107 \\ 157.759 \\ -465.448 \\ 766.573 \\ -610.957 \\ 183.935 \end{bmatrix}$$

$v_{f_k} := v\left(z_{f_k}\right)$ degree := 5 i := 0.. degree point := 0.. Rows

$z\,matrix_{(point,i)} := \left[z_{f_{(point,0)}}\right]^i$ $v_{f\_coeff} := \left(z\,matrix^T \cdot z\,matrix\right)^{-1} \cdot z\,matrix^T \cdot v_f$

$v_{f\_eq}(z) := \left(\sum_i v_{f\_coeff_i} \cdot z^i\right) \cdot N$

Shear

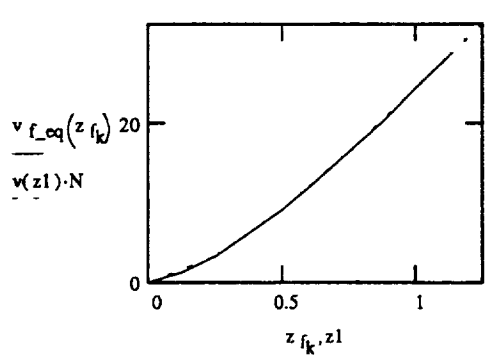

$$v_{f\_coeff} = \begin{bmatrix} -0.003 \\ 5.102 \\ 42.577 \\ -44.308 \\ 28.794 \\ -8.037 \end{bmatrix}$$

$M_{f_k} := M\left(z_{f_k}\right)$ degree := 5 i := 0.. degree point := 0.. Rows

$z\,matrix_{(point,i)} := \left[z_{f_{(point,0)}}\right]^i$ $M_{f\_coeff} := \left(z\,matrix^T \cdot z\,matrix\right)^{-1} \cdot z\,matrix^T \cdot M_f$

$M_{f\_eq}(z) := \left(\sum_i M_{f\_coeff_i} \cdot z^i\right) \cdot N \cdot m$

Moment

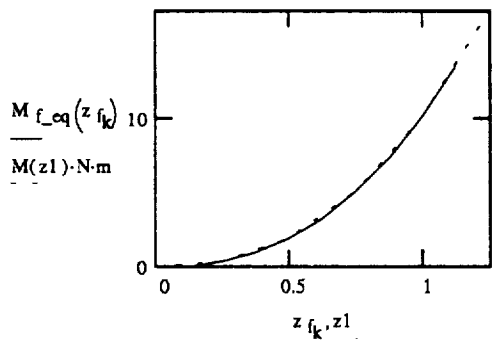

$$M_{f\_coeff} = \begin{bmatrix} 2.685 \cdot 10^{-4} \\ -0.147 \\ 3.784 \\ 10.055 \\ -4.587 \\ 0.974 \end{bmatrix}$$

Airfoil Coordinates Of the HPRS-33

x_u	y_u	y_l	x_l
0	0	0	0
0.00182	0.01182	-0.0086	0.00182
0.00455	0.0185	-0.01275	0.00455
0.01136	0.0279	-0.01812	0.01136
0.02273	0.03786	-0.02377	0.02273
0.03409	0.04522	-0.02818	0.03409
0.04545	0.05091	-0.03152	0.04545
0.06818	0.05965	-0.03717	0.06818
0.09091	0.06645	-0.04151	0.09091
0.11364	0.0719	-0.04493	0.11364
0.13636	0.07648	-0.04792	0.13636
0.15909	0.08044	-0.05034	0.15909
0.18182	0.08372	-0.05134	0.18182
0.22727	0.08889	-0.05234	0.22727
0.27273	0.09245	-0.05234	0.27273
0.31818	0.09463	-0.05234	0.31818
0.36364	0.09545	-0.05234	0.36364
0.42209	0.09505	-0.05234	0.42209
0.46755	0.09335	-0.05234	0.46755
0.513	0.09015	-0.05234	0.513
0.53573	0.0877	-0.05134	0.53573
0.55845	0.08522	-0.05019	0.55845
0.58118	0.08194	-0.04766	0.58118
0.60391	0.07822	-0.0447	0.60391
0.62664	0.07404	-0.04132	0.62664
0.64936	0.06945	-0.03767	0.64936
0.67209	0.06451	-0.03383	0.67209
0.69482	0.05925	-0.02988	0.69482
0.71755	0.05375	-0.02588	0.71755
0.74027	0.04745	-0.02174	0.74027
0.763	0.04222	-0.01793	0.763
0.78573	0.03621	-0.01402	0.78573
0.80845	0.03012	-0.01052	0.80845
0.83118	0.02399	-0.00752	0.83118
0.85391	0.01875	-0.0055	0.85391
0.87664	0.01363	-0.00466	0.87664
0.89936	0.00951	-0.00466	0.89936
0.91559	0.007	-0.00475	0.91559
0.93182	0.005	-0.0042	0.93182
0.94319	0.00425	-0.004	0.94319
0.95455	0.00375	-0.0038	0.95455
0.96591	0.0033	-0.003	0.96591
0.97727	0.00415	-0.001	0.97727
0.98864	0.0055	0.001	0.98864

$\begin{bmatrix} 0.999 \\ 1 \end{bmatrix}$ $\begin{bmatrix} 0.007 \\ 0.005 \end{bmatrix}$ $\begin{bmatrix} 0.003 \\ 0.005 \end{bmatrix}$ $\begin{bmatrix} 0.999 \\ 1 \end{bmatrix}$

Geometric Parameters

$i := 0..45$ $j := 0..44$ $KPa \equiv 1000 \cdot Pa$

Span	$s := 1.25 \cdot m$
Chord Lenght	$cord := 0.455 \cdot m$
Engine Weight	$w_e := 5.719 \cdot N$
Cross Sectional Area of Engine	$A_e := (0.0455 \cdot m)^2 \cdot \pi$ $A_e = 0.007 \cdot m^2$
Distance of Engine from the root chord	$d := 57 \cdot cm$
Center of Gravity of the Engine	$X_{ecg} := -0.017 \cdot m$ $Y_{ecg} := 0.006 \cdot m$
Thrust	$T := \frac{50}{30} \cdot N$
Wing Sweep	$\beta := 0 \cdot deg$
Drag of Wing	$D := 0.109 \cdot N$
Moment Due to Drag	$M_D := \frac{D}{4} \cdot (s)$ $M_D = 0.034 \cdot m \cdot N$
Center of Gravity	$X_{cg} := 0.113 \cdot m$ $Y_{cg} := 0.006 \cdot m$
Airfoil Coordinates Upper	$X_{a_i} := x_{u_i} \cdot cord$ $Y_{u_i} := y_{u_i} \cdot cord$
Lower	$Y_{l_i} := y_{l_i} \cdot cord$
Wing Center of Gravity	$X_{wcg} := 0.209 \cdot m$ $Y_{wcg} := 0.00561 \cdot m$

Calculated Cross Sectional Area at Root

$$A_{ws} := \sum_j \left[\left(Y_{u_j} - Y_{l_j} \right) + \left[Y_{u_{(j+1)}} - Y_{l_{(j+1)}} \right] \right] \cdot \frac{\left[X_{a_{(j+1)}} - X_{a_j} \right]}{2} \qquad A_{ws} = 0.02 \cdot m^2$$

Moment of inertia about the x-axis upper

$$I_{wx1} := \sum_j \left[\left(Y_{u_j} \right)^2 \cdot \left[Y_{u_{(j)}} + Y_{u_{(j+1)}} \right] \right] \cdot \frac{\left[X_{a_{(j+1)}} - X_{a_j} \right]}{2} \qquad I_{wx1} = 1.772 \cdot 10^{-5} \cdot m^4$$

Moment of inetrtia about the x-axis lower

$$I_{wx2} := \sum_j \left[\left(Y_{l_j} \right)^2 \cdot \left[Y_{l_{(j)}} + Y_{l_{(j+1)}} \right] \right] \cdot \frac{\left[X_{a_{(j+1)}} - X_{a_j} \right]}{2} \qquad I_{wx2} = -3.314 \cdot 10^{-6} \cdot m^4$$

Moment of inertia about the y-axis upper

$$I_{wy1} := \sum_j \left[\left(X_{a_j} \right)^2 \cdot \left[Y_{u_{(j)}} + Y_{u_{(j+1)}} \right] \right] \cdot \frac{\left[X_{a_{(j+1)}} - X_{a_j} \right]}{2} \qquad I_{wy1} = 5.537 \cdot 10^{-4} \cdot m^4$$

Moment of inertia about the y-axis lower

$$I_{wy2} := \sum_j \left[\left(X_{a_j} \right)^2 \cdot \left[Y_{l_{(j)}} + Y_{l_{(j+1)}} \right] \right] \cdot \frac{\left[X_{a_{(j+1)}} - X_{a_j} \right]}{2} \qquad I_{wy2} = -2.836 \cdot 10^{-4} \cdot m^4$$

Total moment of inertia of the wing about x-axis

$$I_{wx} := \left| I_{wx1} \right| + \left| I_{wx2} \right| + A_{ws} \cdot \left(0 \cdot m - Y_{wcg} \right)^2 \qquad I_{wx} = 2.168 \cdot 10^{-5} \cdot m^4$$

Total moment of inertia of the wing about y-axis

$$I_{wy} := \left| I_{wy1} \right| + \left| I_{wy2} \right| + A_{ws} \cdot \left(0 \cdot m - X_{wcg} \right)^2 \qquad I_{wy} = 0.002 \cdot m^4$$

Total moment of inertia about x-axis

$$I_x := I_{wx} + A_{ws} \cdot \left(Y_{cg} - Y_{wcg} \right)^2 + A_e \cdot \left(Y_{cg} - Y_{ecg} \right)^2 \qquad I_x = 2.168 \cdot 10^{-5} \cdot m^4$$

Total moment of inertia about x-axis

$$I_y := I_{wy} + A_{ws} \cdot \left(X_{cg} - X_{wcg} \right)^2 + A_e \cdot \left(X_{cg} - X_{ecg} \right)^2 \qquad I_y = 0.002 \cdot m^4$$

Stress on lower surface

$$\sigma_{1_i} := \frac{-\left[\left(M_{f\_eq}\left(\frac{s}{m}\right) - w_e \cdot d\right)\cdot\left(Y_{l_i} - Y_{cg}\right)\right]}{I_x} + \frac{\left[\left(M_D - T\cdot\cos(\beta)\cdot d\right)\cdot\left(X_{a_i} - X_{cg}\right)\right]}{I_y} - \frac{(T\cdot\sin(\beta))}{A_{ws}}$$

Stress on upper surface

$$\sigma_{2_i} := \frac{-\left[\left(M_{f\_eq}\left(\frac{s}{m}\right) - w_e \cdot d\right)\cdot\left(Y_{u_i} - Y_{cg}\right)\right]}{I_x} + \frac{\left[\left(M_D - T\cdot\cos(\beta)\cdot d\right)\cdot\left(X_{a_i} - X_{cg}\right)\right]}{I_y} - \frac{(T\cdot\sin(\beta))}{A_{ws}}$$

Stress On Lower Surface

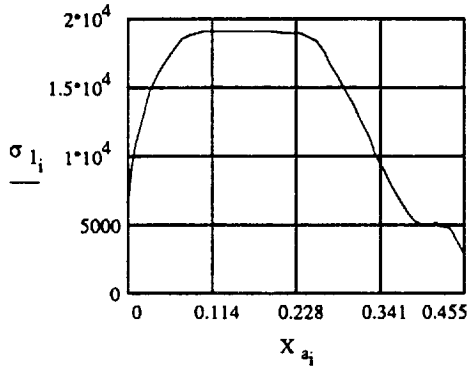

Stress On Upper Surface

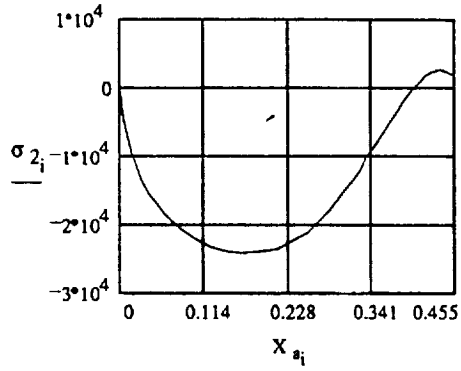

$$\sigma_1 = \begin{vmatrix} 3.892 \\ 6.397 \\ 7.605 \\ 9.168 \\ 10.812 \\ 12.094 \\ 13.064 \\ 14.705 \\ 15.965 \\ 16.957 \\ 17.823 \\ 18.523 \\ 18.81 \\ 19.092 \\ 19.082 \\ 19.073 \\ 19.064 \\ 19.052 \\ 19.042 \\ 19.033 \\ 18.737 \\ 18.397 \\ 17.656 \\ 16.789 \\ 15.799 \\ 14.732 \\ 13.608 \\ 12.453 \\ 11.283 \\ 10.073 \\ 8.958 \\ 7.815 \\ 6.79 \\ 5.912 \\ 5.319 \\ 5.069 \\ 5.065 \\ 5.088 \\ 4.924 \\ 4.863 \\ 4.803 \\ 4.567 \\ 3.983 \\ 3.398 \\ 2.813 \\ 2.23 \end{vmatrix} \cdot KPa \qquad \sigma_2 = \begin{vmatrix} 3.892 \\ 0.449 \\ -1.498 \\ -4.237 \\ -7.141 \\ -9.287 \\ -10.947 \\ -13.497 \\ -15.483 \\ -17.075 \\ -18.414 \\ -19.572 \\ -20.532 \\ -22.047 \\ -23.094 \\ -23.738 \\ -23.986 \\ -23.882 \\ -23.396 \\ -22.473 \\ -21.764 \\ -21.046 \\ -20.096 \\ -19.017 \\ -17.804 \\ -16.471 \\ -15.037 \\ -13.51 \\ -11.912 \\ -10.082 \\ -8.563 \\ -6.817 \\ -5.048 \\ -3.267 \\ -1.745 \\ -0.258 \\ 0.937 \\ 1.665 \\ 2.244 \\ 2.46 \\ 2.604 \\ 2.732 \\ 2.482 \\ 2.087 \\ 1.648 \\ 2.23 \end{vmatrix} \cdot KPa$$

Deflection Angle

$a0 := M_{f\_coeff_0} \cdot N \cdot m$ $\quad a3 := M_{f\_coeff_3} \cdot N \cdot m$ $\quad M_{we} := w_e \cdot d$

$a1 := M_{f\_coeff_1} \cdot N \cdot m$ $\quad a4 := M_{f\_coeff_4} \cdot N \cdot m$

$a2 := M_{f\_coeff_2} \cdot N \cdot m$ $\quad a5 := M_{f\_coeff_5} \cdot N \cdot m$

Moment Equation: $Mo(x) := a5 \cdot x^5 + a4 \cdot x^4 + a3 \cdot x^3 + a2 \cdot x^2 + a1 \cdot x + a0 + M_{we}$

$$\theta 1(x) = \frac{1}{2} \cdot a1 \cdot x^2 + a0 \cdot x + \frac{1}{4} \cdot a3 \cdot x^4 + \frac{1}{3} \cdot a2 \cdot x^3 + \frac{1}{6} \cdot a5 \cdot x^6 + \frac{1}{5} \cdot a4 \cdot x^5 - M_{we} \cdot x + C1$$

$$\theta 1(x) := \frac{1}{2} \cdot a1 \cdot x^2 + a0 \cdot x + \frac{1}{4} \cdot a3 \cdot x^4 + \frac{1}{3} \cdot a2 \cdot x^3 + \frac{1}{6} \cdot a5 \cdot x^6 + \frac{1}{5} \cdot a4 \cdot x^5 - M_{we} \cdot x$$

$$y(x) = \frac{1}{42} \cdot a5 \cdot x^7 + \frac{1}{12} \cdot a2 \cdot x^4 + \frac{1}{6} \cdot a1 \cdot x^3 + \frac{1}{30} \cdot a4 \cdot x^6 + \frac{1}{20} \cdot a3 \cdot x^5 + \frac{1}{2} \cdot a0 \cdot x^2 - \frac{1}{2} \cdot M_{we} \cdot x^2 + C1 \cdot x + C2$$

$C1 := -\theta 1\left(\frac{s}{m}\right)$ $\quad C1 = -2.231 \cdot m \cdot N$

$$y1(x) := \frac{1}{42} \cdot a5 \cdot x^7 + \frac{1}{12} \cdot a2 \cdot x^4 + \frac{1}{6} \cdot a1 \cdot x^3 + \frac{1}{30} \cdot a4 \cdot x^6 + \frac{1}{20} \cdot a3 \cdot x^5 + \frac{1}{2} \cdot a0 \cdot x^2 + C1 \cdot x - \frac{1}{2} \cdot M_{we} \cdot x^2$$

$C2 := -y1\left(\frac{s}{m}\right)$ $\quad C2 = 3.551 \cdot m \cdot N$

$$y(x) := \frac{1}{42} \cdot a5 \cdot x^7 + \frac{1}{12} \cdot a2 \cdot x^4 + \frac{1}{6} \cdot a1 \cdot x^3 + \frac{1}{30} \cdot a4 \cdot x^6 + \frac{1}{20} \cdot a3 \cdot x^5 + \frac{1}{2} \cdot a0 \cdot x^2 - \frac{1}{2} \cdot M_{we} \cdot x^2 + C1 \cdot x + C2$$

$x := \frac{s}{m}, \frac{s}{m} - 0.01 .. 0$

Dihedral*

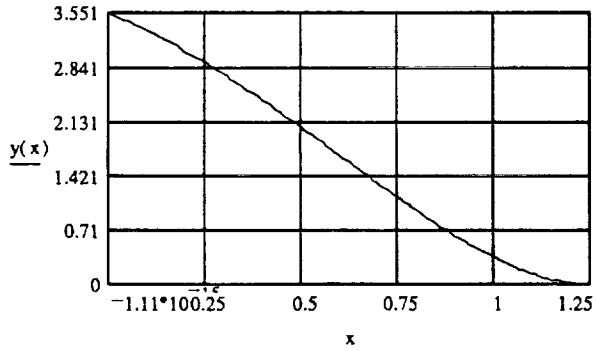

*Mesurment of Dihedral is not devided by E, the modulus of elasticity of the carbon fiber and I, the moment of inertia of the wing

Shear Flow

Shear flow analysis modeled as a closed loop section.
Assuming counterclock-wise direction is positive

$carbon_{thick} := 0.05 \cdot 10^{-2} \cdot m$ $\quad w_e = 5.719 \cdot N$ $\quad x_{cp} := 0.111 \cdot m$ $\quad Lift := Lift \cdot N$

$$\tau := \frac{w_e \cdot X_{ecg} - \frac{Lift}{2} \cdot x_{cp}}{2 \cdot A_{ws} \cdot carbon_{thick}} \qquad \tau = -1.837 \cdot 10^{5} \cdot m^{-2} \cdot N$$

APPENDIX F

INVISID VORTEX PANEL CODE

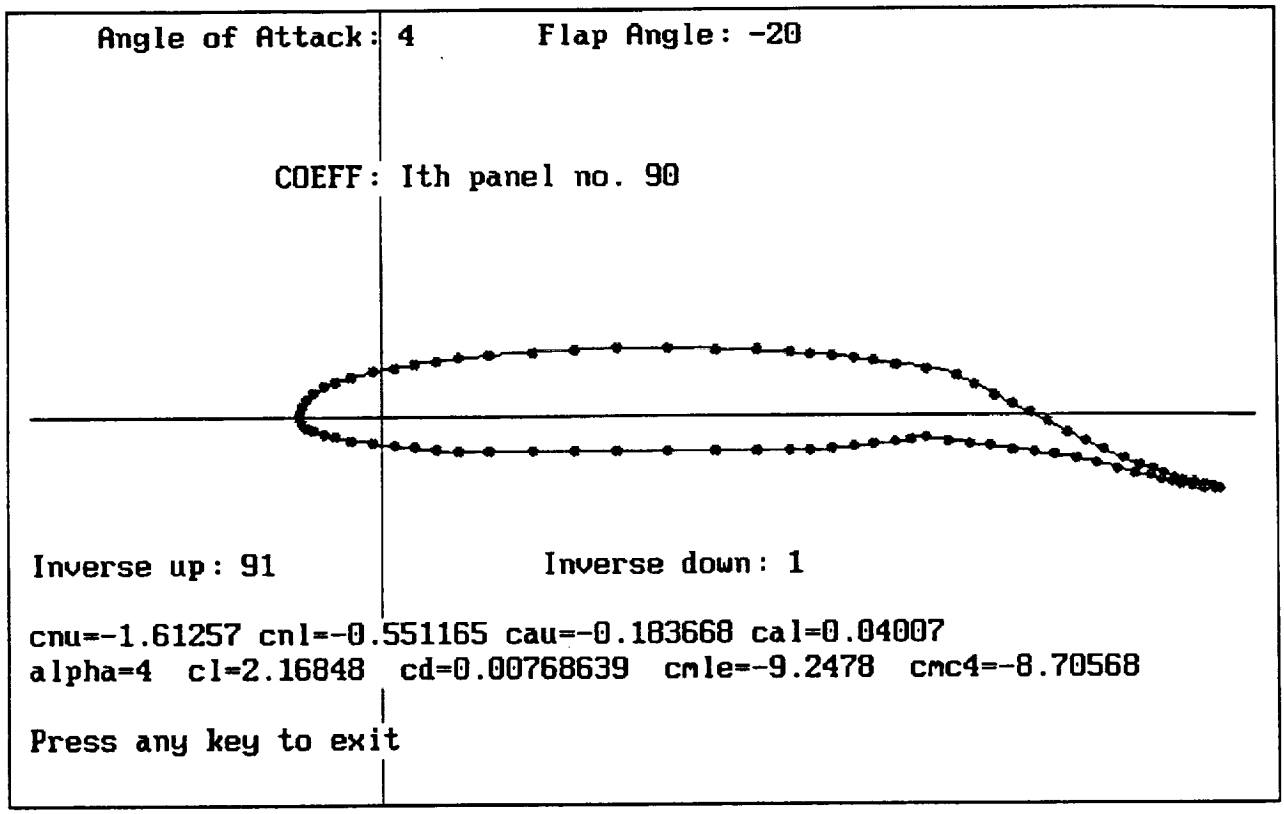

This program uses an inviscid method to solve for the velocity and pressure coefficient distribution over an airfoil shape. The program requires a file which contains the airfoil coordinates **starting at the trailing edge on the lower side** and then proceeding around the airfoil all the way back to the to the starting point. The second file is angle.dat which contains the angles of attack for the airfoil. If flap deflection is required a file with the flap deflection angles is needed. The program produces two files cp.out, and vr.int. The first contains the coefficient of pressure distribution over the airfoil and the second contains the lift drag and moment coefficient.

```
/*************************************************************
*************************************************************
************** Program Vortex.c  ***********************
************** December 1992     ***********************
************** Yuri Zhovnirovsky, Shilpa Shroff ********
*************************************************************
*************************************************************/
#include <stdio.h>
#include <malloc.h>
#include <stdlib.h>
#include <math.h>
#include <conio.h>
#include <graphics.h>
#include "c:\mqp\mv.c"        /* Numerical Recipes Dynamic Memory Allocation */
#include "c:\mqp\inverse.c"  /* Calculates an inverse of a matrix */

#define FALSE 0
#define TRUE 1

float PI;
int             GraphDriver;   /* graphics variables for the initialization of */
int         GraphMode;         /* graphics screen */

/* This procedure solves a system of linear equations
   c - Contains the variable coefficients (left hand side)
   a - Right hand side
   x - Solution vector
   n - Number of equations
*/
void solve(c, a, x, n)
float **c, *a, *x;
int       n;
{
float           **cc;
register int     i,j,k;

     cc=matrix(1,n,1,n);
     inverse(c,cc,n,n);
     mproduct(cc,a,x,n,n,n,1);
     free_matrix(cc,1,n,1,n);
}

/* This procedure integrated the pressure coefficient in order
   to determine the Lift, Drag and Moment about the quater chord
   point.
   fp       - file pointer for output.
   x,y      - panel mid point coordinates
   xb, yb   - panel end point coordinates
   s        - panel lenght
   cp       - pressure coefficient
   th       - angle of panel
   M        - number of panels
   mid_point - Separation point between upper and lower surface
   alpha    - angle of attack
*/
void integ(fp,x,y,xb,yb,s,cp,th,M,mid_point,alpha)
FILE  *fp;
float *x, *y, *xb, *yb, *s, *cp, *th;
int       M, mid_point;
float alpha;
{
register int     j,k;
int              M2;
float            cn, ca, cmle, cmc4, cnl, cnu, cal, cau, cl, cd;
float            q_inf=137.99, p_inf=101325.0;
```

```
    cau=0;    cal=0;
    cnu=0;    cnl=0;
    cmle=0;
    M2=mid_point;
    for (j=1; j<M2; j++){
        cnl=cnl+cp[j]*s[j]*cos(th[j]);
        cal=cal+cp[j]*s[j]*sin(th[j]);
        cmle=cmle-(p_inf+cp[j]*q_inf) * s[j] / q_inf *
                (x[j]*cos(PI-th[j]) + fabs(y[j]) * sin(PI-th[j]));
    }

    for (j=M2; j<=M; j++){
        cnu=cnu+cp[j]*s[j]*cos(th[j]);
        cau=cau+cp[j]*s[j]*sin(th[j]);
        cmle=cmle+(p_inf+cp[j]*q_inf) * s[j] / q_inf *
                (x[j]*cos(th[j]) + fabs(y[j]) * sin(th[j]));
    }

    printf("cnu=%g cnl=%g cau=%g cal=%g              \n",cnu,cnl,cau,cal);
    cn=-cnu-cnl;
    ca=cau+cal;
    cl=cn*cos(alpha)-ca*sin(alpha);
    cd=cn*sin(alpha)+ca*cos(alpha);
    cmc4=cmle+cl/4.0;
    printf("alpha=%g  cl=%g  cd=%g  cmle=%g  cmc4=%g                \n",
                                alpha*180/PI, cl, cd, cmle, cmc4);
    fprintf(fp,"%g, %g, %g, %g, %g\n",alpha*180/PI, cl, cd, cmle, cmc4);
}

/* Scans the input file to determine the number of panels.
   Also determines the position of the inflection point between
   the upper and lower surface
   fp  - File pointer
   mid - mid point (return vector)
   Procedure returns the number of panels.
*/
int scan_file(fp, mid)
FILE    *fp;
int     *mid;
{
int     i;
float xa, xa_old, ya;

    i=1;
    *mid=-1;
    while((fscanf(fp,"%f %f",&xa, &ya))!=EOF){
        if (i==1)
            xa_old=xa;
        if (((xa_old-xa)<0.0) && (*mid<0))
            *mid=i-1;
        xa_old=xa;
        i++;
    }
    fclose(fp);
    return(i-1);
}

/* Read in the panels from the file
   fp  - File pointer
   x_p - x coordinate
   y_p - y coordinate
*/
void getpanels(fp,x_p,y_p)
FILE    *fp;
float   *x_p, *y_p;
```

```
{
int         i;
float xa, ya;

     i=1;
     while(((fscanf(fp,"%f %f",&xa,&ya))!=EOF)){
          x_p[i]=xa;
          y_p[i]=ya;
          i++;
     }
     fclose(fp);
}

/* Rotate preforms a 2-D rotation of the airfoil coordinates
   about the a certain percent of the chord. It only rotates the
   points which are after this percentage. This is done to allow
   for flap deflection analysis.
   r           - Degrees of rotation
   x_in, y_in  - input x, y coordinate vector
   x_out, y_out - rotated x, y coordinate output vector
   p_chord     - percent of chord to rotate about
   Mp          - Number of panels
*/
void rotate(r, x_in, y_in, x_out, y_out, p_chord, Mp)
float             r, *x_in, *y_in, *x_out, *y_out, p_chord;
int         Mp;
{
float z_matrix[3][3];
float xu_o, yu_o, xl_o, yl_o;
int   i, first_pass;

/* Z matrix
**
**  | cos A  -sin A   0  |
**  | sin A   cos A   0  |
**  | 0          0    1  |
**
*/


     z_matrix[0][0]=cos(r);
     z_matrix[0][1]=-sin(r);

     z_matrix[1][0]=sin(r);
     z_matrix[1][1]=cos(r);

     i=1;
     xu_o=-10;    yu_o=-10;
     xl_o=-10;    yl_o=-10;

     p_chord=1-p_chord;
     while ((i<Mp+1) && (yu_o==-10)){
          if ((x_in[i]<=p_chord) && (xl_o==-10)){
               xl_o=x_in[i-1];
               yl_o=y_in[i-1];
          }
          if ((x_in[i]>=p_chord) && (xl_o!=-10)){
               xu_o=x_in[i];
               yu_o=y_in[i];
          }
          i++;
     }
     for (i=1; i<=Mp+1; i++){
          if (x_in[i]>=p_chord){
               if (i<Mp/2){
```

```
                    x_out[i]=xl_o+(x_in[i]-xl_o) * z_matrix[0][0] +
                                (y_in[i]) * z_matrix[0][1];
                    y_out[i]=(x_in[i]-xl_o) * z_matrix[1][0] +
                                (y_in[i]) * z_matrix[1][1];
               }
               else{
                    x_out[i]=xu_o+(x_in[i]-xu_o) * z_matrix[0][0] +
                                (y_in[i]) * z_matrix[0][1];
                    y_out[i]=(x_in[i]-xu_o) * z_matrix[1][0] +
                                (y_in[i]) * z_matrix[1][1];
               }
          }
          else{
               x_out[i]=x_in[i];
               y_out[i]=y_in[i];
          }
     }
}

/* Create Graphical output */
void do_graphics(M,xb,yb,x,y)
int   M;
float *xb, *yb, *x, *y;
{
int   i;
float y_f, x_f, x_o, y_o;

     y_f=(float)getmaxy()/1.5;
     x_f=(float)getmaxx()/1.5;
     x_o=x_f/3.5;
     y_o=y_f/1.4;
     setcolor(RED);
     line(0, y_o, getmaxx(), y_o);
     line(getmaxx()/4, 0, getmaxx()/4, getmaxy());
     setcolor(GREEN);
     for (i=2; i<=M+1; i++){
          setcolor(BLUE);
          setfillstyle(SOLID_FILL, YELLOW);
          if (i<=M)
               fillellipse(x[i]*x_f+x_o, -y[i]*y_f+y_o, 2, 2);

          setcolor(GREEN);
          line(xb[i-1]*x_f+x_o,-yb[i-1]*y_f+y_o,xb[i]*x_f+x_o,-yb[i]*y_f+y_o);
     }
     line(xb[1]*x_f+x_o,-yb[1]*y_f+y_o,xb[M+1]*x_f+x_o,-yb[M+1]*y_f+y_o);
}


void main(){
register int     i,j,k;
int              M, mp1, ip1, mid_point;
short int        do_flaps;
float            angle, flap_angle, p_ch;
FILE             *fp, fp_out, *fp_int, *fp_angle;
char             filename_air[15], filename[15], ch;
float            A, B, C, D, E, F, G, P, Q, alpha;
float            *xb, *yb, *xb1, *yb1, *x, *y, *s, *sine, *cosine,
                      *theta, *v, *cp, *rhs, *gama, **cn1,
                      **cn2, **ct1, **ct2, **an, **at;

     clrscr();
     do_flaps=FALSE;

     printf("Enter input file name: ");
     scanf("%s",filename_air);
```

```
fflush(stdin);
fp=fopen(filename_air,"r");
if (fp==NULL){
     printf("FILE NOT FOUND\n");
     exit(-1);
}
printf("Do you wish to deflect the flap: [y/n]");
ch=getch();
if ((ch=='y') || (ch=='Y')){
     printf("\n  Enter the file name with the flap deflection: ");
     scanf("%s",filename);
     fflush(stdin);
     fp_angle=fopen(filename,"r");
     if (fp_angle==NULL){
          printf("ERROR: Flap file not found\n");
          exit(-1);
     }
     printf("\n  Enter the angle of attack: ");
     scanf("%f",&flap_angle);
     fflush(stdin);
     printf("\n  Enter the size of the flap in percent chord: ");
     scanf("%f",&p_ch);
     fflush(stdin);
     p_ch=p_ch/100.0;
     do_flaps=TRUE;
}
else
     printf("\n");

M=scan_file(fp, &mid_point);
fp=fopen(filename_air,"r");

/* Allocate memory for coordinates */
xb1=vector(1,M);
yb1=vector(1,M);
xb=vector(1,M);
yb=vector(1,M);
M--;
printf("Using %d panels\n",M);

getpanels(fp,xb1,yb1);              /* Read in the panels */

/* Allocate memory */
x=vector(1,M);
y=vector(1,M);
s=vector(1,M);
sine=vector(1,M);
cosine=vector(1,M);
theta=vector(1,M);
rhs=vector(1,mp1);
PI=4.0*atan(1.0);
mp1=M+1;
sprintf(filename,"vr.int");
fp_int=fopen(filename,"w");          /* open output file vr.int
                                        This file will contain the
                                        integrated cp values */

fp=fopen("cp.out","w");              /* Open output file cp.out This will
                                        contain the raw cp values */

if (!do_flaps){
     fp_angle=fopen("angle.dat","r");
     if (fp_angle==NULL){
          printf("ERROR: The file (angle.dat) which contains the angles of attack is not found\n");
          exit(0);
     }
```

```
}
angle=0.0;
/* rotate if needed */
rotate(angle, xb1, yb1, xb, yb, p_ch, M);
/* Start Graphics */
GraphDriver = DETECT;
initgraph(&GraphDriver, &GraphMode, "c:\\borlandc\\bgi");

/* Read in flap defection if needed */
while(fscanf(fp_angle,"%f",&angle)!=EOF){
    alpha=angle*PI/180.0;
    if (do_flaps){
        gotoxy(30,4); printf("Flap Angle: %g    ",angle);
        rotate(alpha, xb1, yb1, xb, yb, p_ch, M);
        alpha=flap_angle*PI/180.0;
    }
    gotoxy(5,4); printf("Angle of Attack: %g    ",alpha*180.0/PI);
    /* Calculate center points x,y length of panel s
       Angle of panel theta, sine and cosine of this angle,
       and the right hand side matrix.
    */
    for (i=1; i<=M; i++){
        ip1=i+1;
        x[i]=0.5*(xb[i]+xb[ip1]);
        y[i]=0.5*(yb[i]+yb[ip1]);
        s[i]=sqrt(pow(xb[ip1]-xb[i], 2)+pow(yb[ip1]-yb[i], 2));
        theta[i]=atan2(yb[ip1]-yb[i], xb[ip1]-xb[i]);
        sine[i]=sin(theta[i]);
        cosine[i]=cos(theta[i]);
        rhs[i]=sin(theta[i]-alpha);
    }
    do_graphics(M,xb,yb,x,y);                    /* Display graphics */
    /* Allocate more memory */
    cn1=matrix(1,M,1,M);
    cn2=matrix(1,M,1,M);
    ct1=matrix(1,M,1,M);
    ct2=matrix(1,M,1,M);

    for (i=1; i<=M; i++){
        gotoxy(15,8); printf("COEFF: Ith panel no. %d    ",i);
        for (j=1; j<=M; j++){
            if (i==j){
                cn1[i][j]=-1.0;
                cn2[i][j]=1.0;
                ct1[i][j]=0.5*PI;
                ct2[i][j]=0.5*PI;
            }
            else{
                /* Calculate coefficient for the integral */

                A = -(x[i]-xb[j])*cosine[j]-(y[i]-yb[j])*sine[j];
                B = pow(x[i]-xb[j], 2)+pow(y[i]-yb[j], 2);
                C = sin(theta[i]-theta[j]);
                D = cos(theta[i]-theta[j]);
                E = (x[i]-xb[j])*sine[j]-(y[i]-yb[j])*cosine[j];
                F = log(1+s[j]*(s[j]+2.0*A)/B);
                G = atan2(E*s[j], B+A*s[j]);
                P = (x[i]-xb[j])*sin(theta[i]-2.0*theta[j])+
                    (y[i]-yb[j])*cos(theta[i]-2.0*theta[j]);
                Q = (x[i]-xb[j])*cos(theta[i]-2.0*theta[j])-
                    (y[i]-yb[j])*sin(theta[i]-2.0*theta[j]);
                cn2[i][j]=D+0.5*Q*F/s[j]-(A*C+D*E)*G/s[j];
                cn1[i][j]=0.5*D*F+C*G-cn2[i][j];
                ct2[i][j]=C+0.5*P*F/s[j]+(A*D-C*E)*G/s[j];
                ct1[i][j]=0.5*C*F-D*G-ct2[i][j];
```

```
            }
        }
    }
    /* Allocate more more more and some more memory */
    an=matrix(1,mp1,1,mp1);
    at=matrix(1,mp1,1,mp1);

    /* Fill in left hand side matrix */
    for (i=1; i<=M; i++){
        an[i][1]=cn1[i][1];
        an[i][mp1]=cn2[i][M];
        at[i][1]=ct1[i][1];
        at[i][mp1]=ct2[i][M];
        for (j=2; j<=M; j++){
            an[i][j]=cn1[i][j]+cn2[i][j-1];
            at[i][j]=ct1[i][j]+ct2[i][j-1];
        }
    }
    an[mp1][1]=1.0;
    an[mp1][mp1]=1.0;
    for (j=2; j<=M; j++)
        an[mp1][j]=0.0;
    rhs[mp1]=0.0;

    /* Free (quickly) some of that allocated memory */
    free_matrix(cn1,1,M,1,M);
    free_matrix(cn2,1,M,1,M);
    free_matrix(ct1,1,M,1,M);
    free_matrix(ct2,1,M,1,M);

    /* allocate memory for solution vector */
    gama=vector(1,mp1);

    /* SOLVE THE EQUATIONS */
    solve(an, rhs, gama, mp1);

    free_matrix(an,1,mp1,1,mp1);
    v=vector(1,M);
    cp=vector(1,M);
    /* Write cp, and velocity to the cp.out file */
    fprintf(fp,"alpha = %g\n",angle);
    for (i=1; i<=M; i++){
        v[i]=cos(theta[i]-alpha);
        for (j=1; j<=mp1; j++){
            v[i]=v[i]+at[i][j]*gama[j];
            cp[i]=1.0-pow(v[i],2);
        }
        fprintf(fp,"%g, %g, %g, %g, %g, %g\n", xb[i], yb[i], x[i], y[i],
                                                    theta[i], cp[i]);
    }
    fprintf(fp,"\n\n");

    /* Integrate the Cp coefficients to determine the lift and drag */
    integ(fp_int,x,y,xb,yb,s,cp,theta,M,mid_point,alpha);

    /* FREE FREE FREE the memory */
    free_matrix(at,1,mp1,1,mp1);
    free_vector(gama,1,mp1);
    free_vector(cp,1,M);
    free_vector(v,1,M);
}
/* Close files */
fclose(fp);
fclose(fp_int);
fclose(fp_angle);
```

```
    /* FREE ALL OF THE TAKEN MEMORY */
    free_vector(x,1,M);
    free_vector(y,1,M);
    free_vector(theta,1,M);
    free_vector(cosine,1,M);
    free_vector(sine,1,M);
    free_vector(rhs,1,mp1);
    free_vector(s,1,M);
    free_vector(xb,1,mp1);
    free_vector(yb,1,mp1);
    free_vector(xb1,1,mp1);
    free_vector(yb1,1,mp1);
    printf("Press any key to exit\n");
    getch();
    closegraph();          /* close graphics */
}



/****************************** INVERSE .C ***********************************/

float inverse(in_matrix,out_matrix,rows,columns)
float **in_matrix, **out_matrix;
int       rows, columns;
{
int       i,c,r,row,column;
float temp, factor;

    if (in_matrix[1][1]==0){/* check if the first entry is zero */
        row=2;
        while (in_matrix[row][1]==0){/* find the next non zero entry */
            row++;
        }
        for (column=1; column<=columns; column++){ /* switch lines around */
            temp=in_matrix[row][column];
            in_matrix[row][column]=in_matrix[row][column];
            in_matrix[row][column]=temp;
        }
    }

    /* create an identty matrix */
    for (row=1; row<=rows; row++)
        for (column=1; column<=columns; column++)
            if (column==row)
                out_matrix[row][column]=1.0;
            else
                out_matrix[row][column]=0.0;

    /* since the inverse matrix must be sqare only one counter is used */
    for (i=1; i<=rows; i++){
    gotoxy(1,19); printf("Inverse up: %d    \n",i);
        /* introduce leading 1's */
        if (in_matrix[i][i]!=1){
            factor=1.0 / in_matrix[i][i];

            for (c=1; c<=columns; c++){
                in_matrix[i][c]=in_matrix[i][c]*factor;
                out_matrix[i][c]=out_matrix[i][c]*factor;
            }
        }

        /* intrudce 0 bellow the leading 1's */
        for (r=i+1; r<=rows; r++){
            if (in_matrix[r][i]!=0){
```

```
                    factor=in_matrix[r][i] / in_matrix[i][i];

                    /* subtract the factor */
                    for (c=1; c<=columns; c++){
                        in_matrix[r][c]=in_matrix[r][c]-factor*in_matrix[i][c];
                        out_matrix[r][c]=out_matrix[r][c]-factor*out_matrix[i][c];
                    }
                }
            }
        }

        for (i=rows; i>=1; i--){
            gotoxy(30,19); printf("Inverse down: %d     \n",i);
            /*introduce 0 above the leading 1's */
            for (r=i-1; r>=1; r--){
                if (in_matrix[r][i]!=0){
                    factor=in_matrix[r][i] / in_matrix[i][i];

        /* subtract the factor */
                    for (c=columns; c>=1; c--){
                        in_matrix[r][c]=in_matrix[r][c]-factor*in_matrix[i][c];
                        out_matrix[r][c]=out_matrix[r][c]-factor*out_matrix[i][c];
                    }
                }
            }
        }
        return(0);
}


float mproduct(in_matrix1, in_matrix2,out_matrix,rows1,columns1, rows2, columns2)
float **in_matrix1, *in_matrix2, *out_matrix;
int         rows1, columns1, rows2, columns2;
{
int row1, row2;

        for (row1=1; row1<=rows1; row1++){
            out_matrix[row1]=0;
            for (row2=1; row2<=rows2; row2++){
                out_matrix[row1]=out_matrix[row1]+
                in_matrix1[row1][row2] * in_matrix2[row2];
            }
        }
        return(0);
}


/***************************** MV.C ***************************/

void nrerror(error_text)
char error_text[];
{
        void exit();

        fprintf(stderr,"Numerical Recipes run-time error...\n");
        fprintf(stderr,"%s\n",error_text);
        fprintf(stderr,"...now exiting to system...\n");
        exit(1);
}



float *vector(nl,nh)
int nl,nh;
{
```

```
        float *v;

        v=(float *)malloc((unsigned) (nh-nl+1)*sizeof(float));
        if (!v) nrerror("allocation failure in vector()");
        return v-nl;
}

float **matrix(nrl,nrh,ncl,nch)
int nrl,nrh,ncl,nch;
{
        int i;
        float **m;

        m=(float **) malloc((unsigned) (nrh-nrl+1)*sizeof(float*));
        if (!m) nrerror("allocation failure 1 in matrix()");
        m -= nrl;

        for(i=nrl;i<=nrh;i++) {
                m[i]=(float *) malloc((unsigned) (nch-ncl+1)*sizeof(float));
                if (!m[i]) nrerror("allocation failure 2 in matrix()");
                m[i] -= ncl;
        }
        return m;
}

void free_vector(v,nl,nh)
float *v;
int nl,nh;
{
        free((char*) (v+nl));
}

void free_matrix(m,nrl,nrh,ncl,nch)
float **m;
int nrl,nrh,ncl,nch;
{
        int i;

        for(i=nrh;i>=nrl;i--) free((char*) (m[i]+ncl));
        free((char*) (m+nrl));
}
```

APPENDIX G

FINAL CONFIGURATION FOR FLYING WING

FINAL CONFIGURATION OF FLYING WING			
Cruise: 15 m/s at 4° angle of attack			
Elliptical Wing:		**Vertical Tail (two)**:	
wing span	2.5 m	height	21.3 cm
root chord	0.455 m	root chord	17.2 cm
aspect ratio	7.0	tip chord	8.00 cm
airfoil	HPRS 33 (custom)	airfoil	SD 8020
cruise lift	53.5 N	**Composite Structure**:	
cruise L/D	19.7	foam core with carbon/epoxy skin	
Control Surfaces:		**Propulsion**:	
ailerons	two	internal combustion ducted fan engines	two
elevator	one	thrust	15.6 N @ 22,000 rpm
rudders	two		

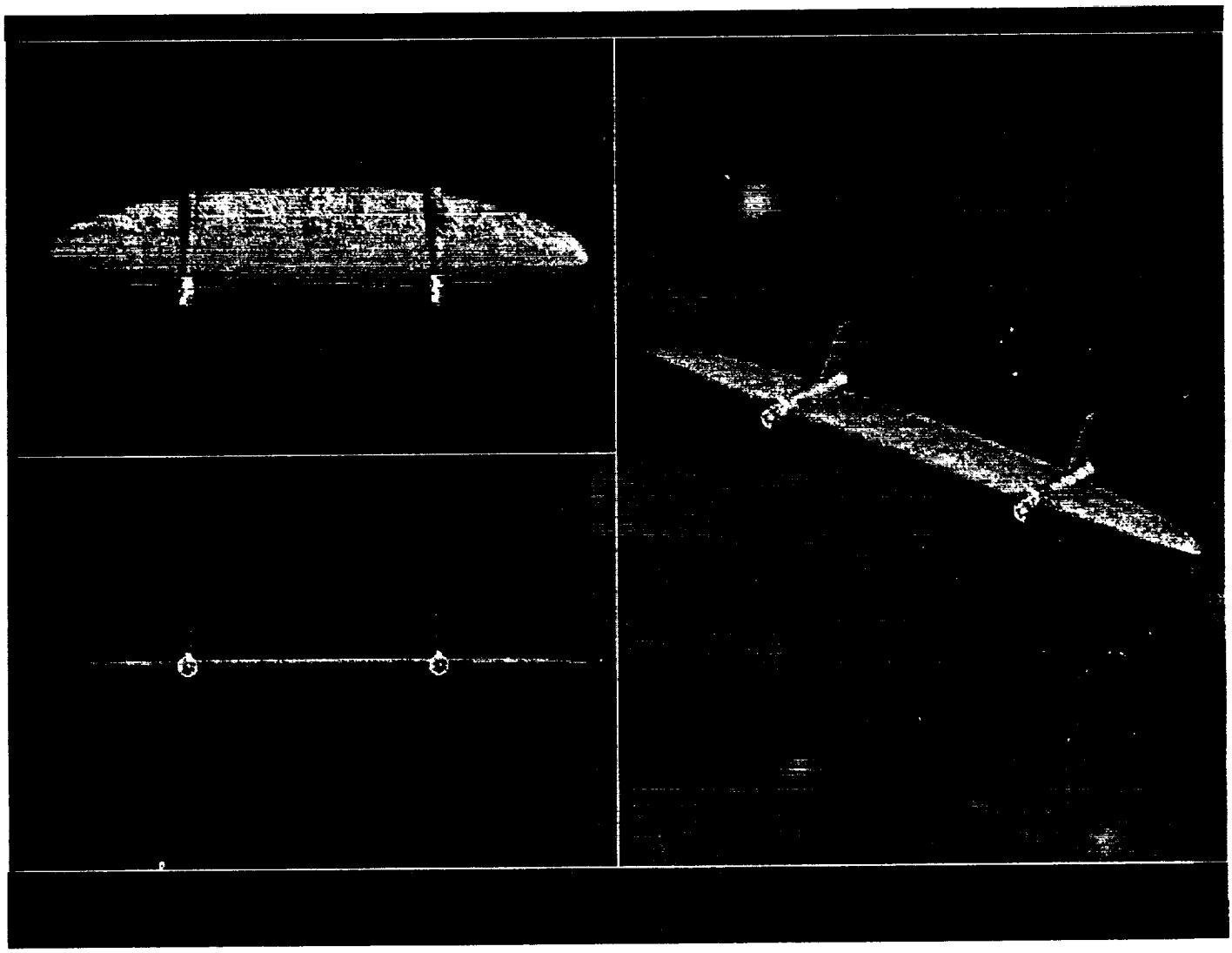

Final Configuration of the Flying Wing